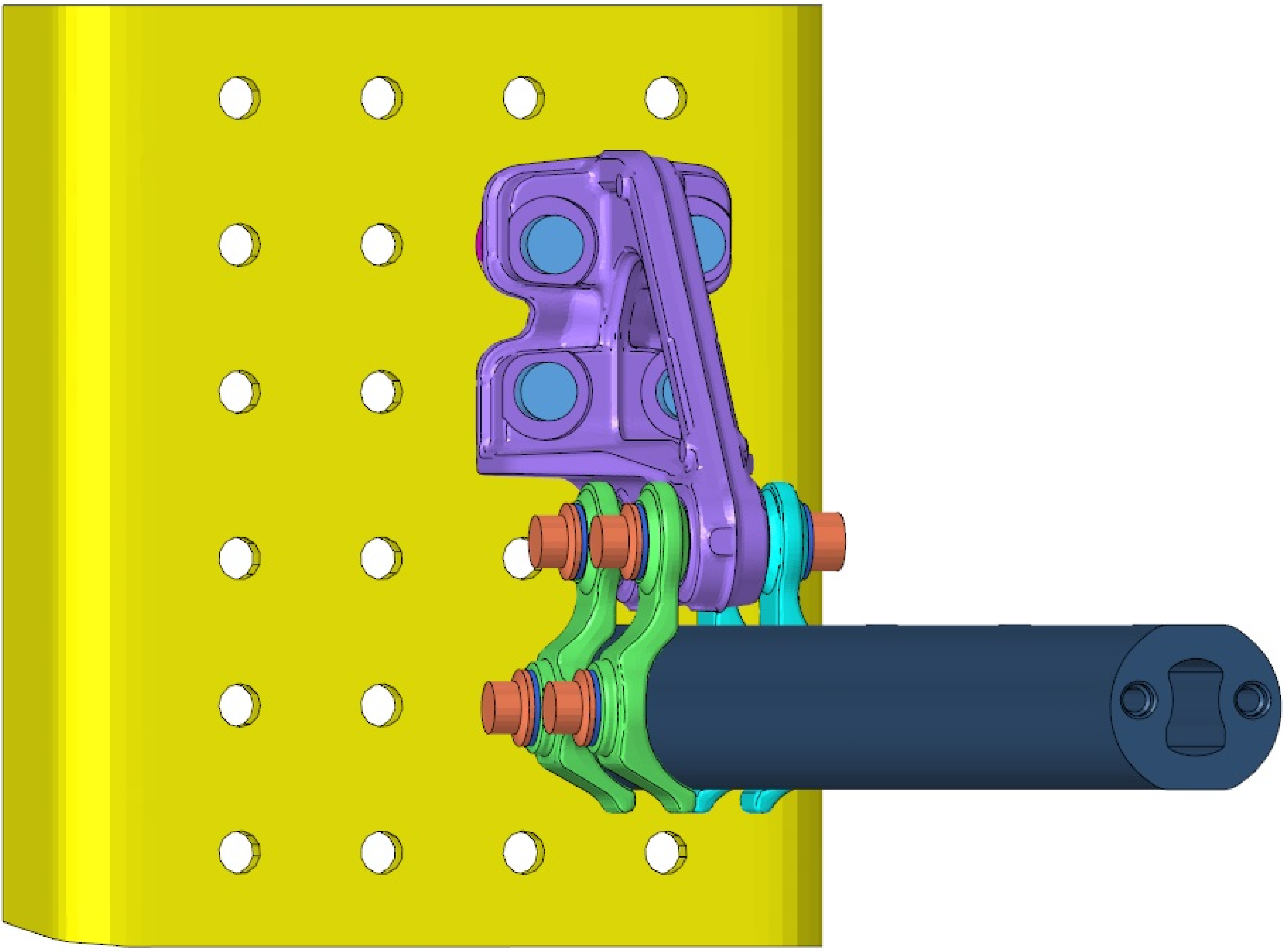

FE-analysis of bolted joints

Correlation between simulation and physical test data

Master's thesis in Applied Mechanics

Magnus Stervik

Department of Mechanics and Maritime Sciences
CHALMERS UNIVERSITY OF TECHNOLOGY
Gothenburg, Sweden 2019

MASTER’S THESIS IN APPLIED MECHANICS

FE-analysis of bolted joints

Correlation between simulation and physical test data

Magnus Stervik

Department of Mechanics and Maritime Sciences
Division of Dynamics
CHALMERS UNIVERSITY OF TECHNOLOGY
Göteborg, Sweden 2019

FE-analysis of bolted joints
Correlation between simulation and physical test data
Magnus Stervik

Master's Thesis 2019:35
Department of Mechanics and Maritime Sciences
Division of Dynamics
Chalmers University of Technology
SE-412 96 Göteborg
Sweden
Telephone: + 46 (0)31-772 1000

Cover:
The simulation model of the mudguard bracket with the joints and the bolts that are being evaluated in the study.

Department of Mechanics and Maritime Sciences
Göteborg, Sweden 2019-06-20

FE-analysis of bolted joints
Correlation between simulation and physical test data
Master's thesis in Applied Mechanics
Magnus Stervik
Department of Mechanics and Maritime Sciences
Division of Dynamics
Chalmers University of Technology

Abstract

A correlation problem was found in a bolted joint when results obtained by physical test were compared to simulation results of a mudguard bracket mounted on a side skirt. The simulation predicts failure in another bolt than the bolt that fails in the physical tests. New rig tests have been performed together with new simulations to find the reason of why the correlation problem is present. The investigation implies that the existing method of evaluating bolted joints capture the overall behavior of the bolts in a good way. However, the new results indicate that the slip of the bolts affects the results to a big extent. The clamping forces together with the friction do play a big part of why the simulation results predicts another outcome of which bolt that fails, when compared to the physical test. The slip that occurs at some of the bolts during the testing causes wear of the clamped components and self-loosening of the bolts which causes great loss of clamping forces. The loss of clamping force is not accounted for in the existing simulation method to the same extent, high axial stresses and bending stresses are therefore obtained in reality which causes failure in the bolts. The slip that is present in the simulation for other of the bolts, do also affect the correlation problem in ways where high bending stresses are found in the simulations compared to the physical tests. The clamping force and the friction coefficient are the two main factors of when slip is initiated, which is difficult to capture in the simulations without measurements. When these two parameters are tuned according to measurements, improved correlation is obtained.

Key words:

Bolted joint, simulation model, rig test, bolt, slip, bending stress, axial stress, friction, wear, axial equivalent stress, bolt evaluation script

FE-analys av skruvförband
Korrelation mellan simuleringar och fysiska tester
Examensarbete inom Tillämpad Mekanik
Magnus Stervik
Institutionen för Mekanik och maritima vetenskaper
Avdelningen för Tillämpad mekanik
Chalmers tekniska högskola

Sammanfattning

Ett korrelationsproblem upptäcktes i ett skruvförband när fysiska provningsresultat jämfördes med resultat erhållna från simuleringar för ett stänkskydd monterat på en sidokjol. Simuleringarna predikterade brott i en annan skruv jämfört med den skruv som fallerade i de fysiska testerna. Nya rigtest har genomförts tillsammans med nya simuleringar med syftet att upptäcka anledningen till korrelationsproblemet. Undersökningen antyder att den nuvarande metoden att evaluera skruvförband fångar det generella beteendet av hur skruvarna beter sig under belastning bra. De nya resultaten uppvisar att korrelationsproblemen till stor utsträckning beror på glidningen i de klämda delarna. Klämkraften tillsammans med friktionen är en anledning till varför simuleringsresultaten inte stämmer överens med provresultaten. Glidningen som uppstår kring vissa av skruvarna under provningen ger upphov till nötning av de klämda delarna samt självlossning av skruvarna vilket leder till stora förluster i klämkraft. Dessa klämkraftsförluster är inte tillräckligt beaktade i den nuvarande simuleringsmetoden. Detta leder till höga axialspänningar samt böjspänningar i vissa skruvar under provningen som leder till skruvbrott, vilket inte fångas i samma utsträckning under simuleringarna. Anledningen till varför korrelationsproblem uppstår för skruv placerade på andra ställen beror också i hög grad på glidning, simuleringar påvisar stor glidning i vissa av de klämda delarna vilket leder till mycket höga böjspänningar i skruven vilket provresultaten inte indikerar. Klämkraft och friktionskoefficienten är de enskilt största anledningarna till när glidning uppstår, detta är två parametrar som är svåra att fånga i simuleringar utan mätningar. När dessa två parametrar i simuleringarna är anpassade efter mätresultaten fås en förbättrad korrelation för skruvarna.

Nyckelord:
Skruvförband, simuleringsmodell, rigtest, skruv, glidning, böjspänning, axialspänning, friktion, nötning, ekvivalent axialspänning, skruvutvärderingsskript

Contents

Preface

I would like to start thanking Thomas Abrahamsson, Professor at Chalmers for all his help during this study.

I would also like to thank Martin Koch for helping me getting started with the project and giving me valuable knowledge of Hypermesh. Thanks to Astrid Cox who performed all the testing and whom without the work would not be achievable. A special thanks to Rickard Österlöf who in times of need came up with new ideas and solutions and was very supportive in the last stages of the study.

At last, big thanks to Maria Lagergren, David Ranger and Niklas Torstensson who has helped me out during the whole thesis and shared their knowledge and supported me through the project with valuable input and ideas to be able to fulfill the thesis. They have all thought me a lot with their experience and expertise through the way they work.

Göteborg March 2019-06-20

Magnus Stervik

1 Introduction

1.1 Background

In 2017 Scania performed a durability test on a side skirt with associated components. During the test, the bolt highlighted in Figure 1, failed before its acceptance criteria were fulfilled. The bolt is located at the joint of the mudguard bracket connecting it to the chassis frame.

In order to evaluate a solution where washers were added to the four bolts connecting the frame bracket to the frame seen in Figure 1, a rig test in the form of a Wöhler test was performed with the failed bolt as the main test specimen together with the relevant parts needed in order to represent the durability test. The evaluation was performed to compare if the fatigue life of the critical bolt would be increased when the clamping length was extended.

A Finite Element (FE) analysis of the mudguard bracket and the bolts was then performed to evaluate the original solution together with the new solution. The results of the analysis did however differ significantly compared to the physical test results.

If the simulation method to evaluate bolted joints does not imply similar outcome as the physical test, the simulation method cannot fully be trusted. For this case, the simulations predict failure in another bolt, this can result in time and resources invested for improving the wrong bolt while the critical bolt is left untouched.

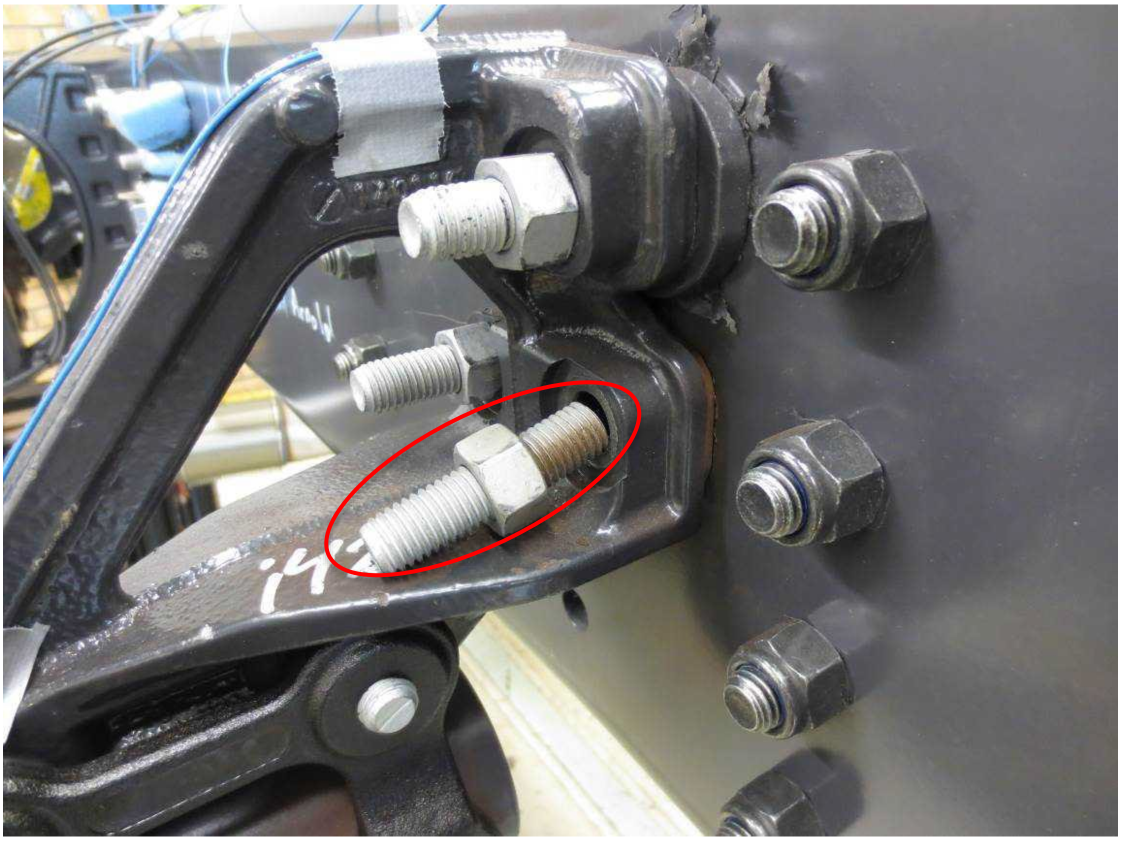

Figure 1: The bolt that failed during the durability test is circled in red.

1.2 Problem statement

Why do the simulation results of the mudguard bracket analysis not correlate with the physical test results?

1.3 Purpose

The study is performed to evaluate the simulation method of bolted joints as it is today. The aim is to find reasons for why the correlation problems between the physical test results and simulations are present and to state suggestions on improvements for the method of evaluating bolted joints.

1.4 Research questions

- Why do the simulation results differ from the physical results?
- Which parameters can be tuned for the simulations in order to improve the correlation?
- What does the existing method of evaluating bolted joint capture and what does it not capture?
- How can the method be improved?

1.5 Scope

- Optimization of the running time for the simulations will not be investigated.
- Understand the tools available for bolt analysis using FEA at Scania and investigate how they were applied for a specific case study.
- Identify shortcomings of current method/knowledge.
- Suggest improvements/developments for the current method.

2 Theory and background

Figure 2: The numbering of the bolts evaluated.

In this chapter a more thorough presentation of results obtained in previous studies is done, together with the theory used for this study.

The naming convention used for the bolts is according to the numbering seen in Figure 2. The bolt that failed during the durability test is with this convention bolt 4. Bolt 5 is the bolt that is critical according to the simulation predictions. The collection name, frame bolts, is used for bolt 1-4, while beam bolts is used for bolt 5-8.

2.1 Background

Data and results obtained by the previous tests and simulations are presented in this chapter.

2.1.1 Wöhler test

The Wöhler test was done for two different cases to compare the results against each other. The first case was with a mudguard bracket without washers, as the original solution in the durability test. The second case was with washers added to the frame bolts. The test was performed with an alternating load applied at the end of the beam seen in Figure 3.

The results of the Wöhler tests obtained from [1] are presented in Table 1 for the case without washers, in Table 2 the results for the case with added washers is seen.

The outcome of the Wöhler test for the case without washers shows that the torque amplitude bolt 4 can withstand for 100 000 cycles is 1.92 kNm. The respective torque amplitude for bolt 4 when washers are added to the frame bolts was calculated to 2.88 kNm.

Table 1: The torque amplitudes, number of cycles to failure and which part that failed for the case without added washers.

Torque amplitude [kNm]	Number of cycles to failure	Failed part
2.98	1 500	Frame bracket
1.86	72 400	Bolt 4
1.64	182 100	Bolt 4
1.50	565 350	Bolt 4

Table 2: The torque amplitudes, number of cycles to failure and which part that failed for the case with added washers.

Torque amplitude [kNm]	Number of cycles to failure	Failed part
1.86	160 800	Frame bracket
1.64	179 600	Bolt 4
1.64	709 300	Runout
1.50	848 200	Runout
1.50	137 200	Runout

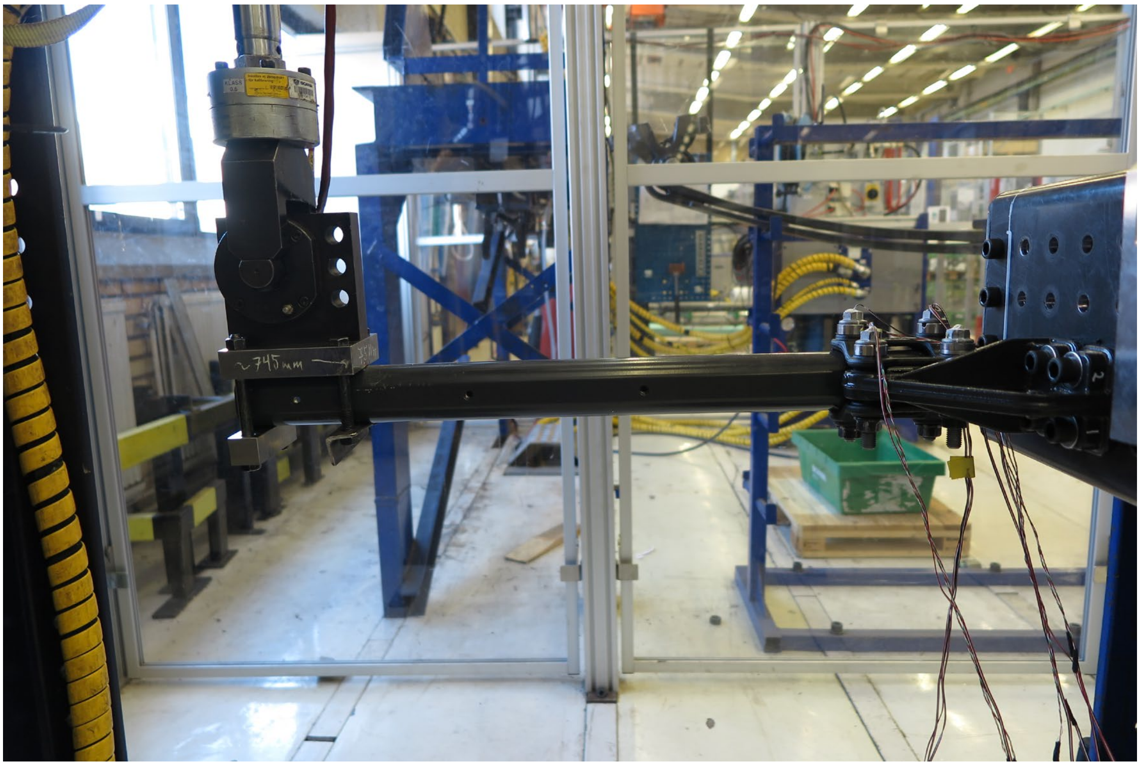

Figure 3: The load is applied from the cylinder at the left end of the beam.

2.1.2 Simulations

The simulation model created to represent the Wöhler test is presented in Figure 4. A load of 3800 N was applied at the end of the beam in the direction seen in the figure. The torque distance is measured from the frame face to the end of the beam with a distance of 0.789m, which results in a torque amplitude of 3 kNm. Linear material models were used and the friction coefficient was set to 0.15 according to standards [2].

The simulation results that will be used for comparison in this project are presented in Figure 5. Bolt 4 should according to the predictions do fail after 100 000 cycles at a torque amplitude of 2.36 kNm. This means that the simulation predicts a 100 000-cycle load that is 23 % lower than the physical test results indicate.

The simulation results predict that bolt 5 fails after 100 000 cycles at a torque amplitude of 1.52 kNm. According to the Wöhler test, should bolt 5 withstand a torque amplitude of 2.88 kNm for 100 000 cycles. The discrepancy for bolt 5 is greater than 50 % compared to the physical test.

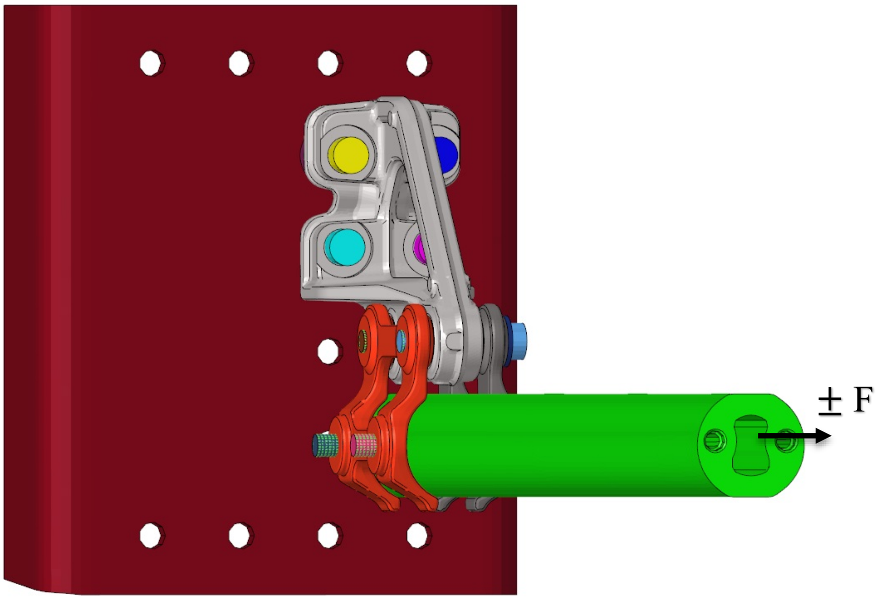

Figure 4: Simulation model used for evaluating the mudguard bracket.

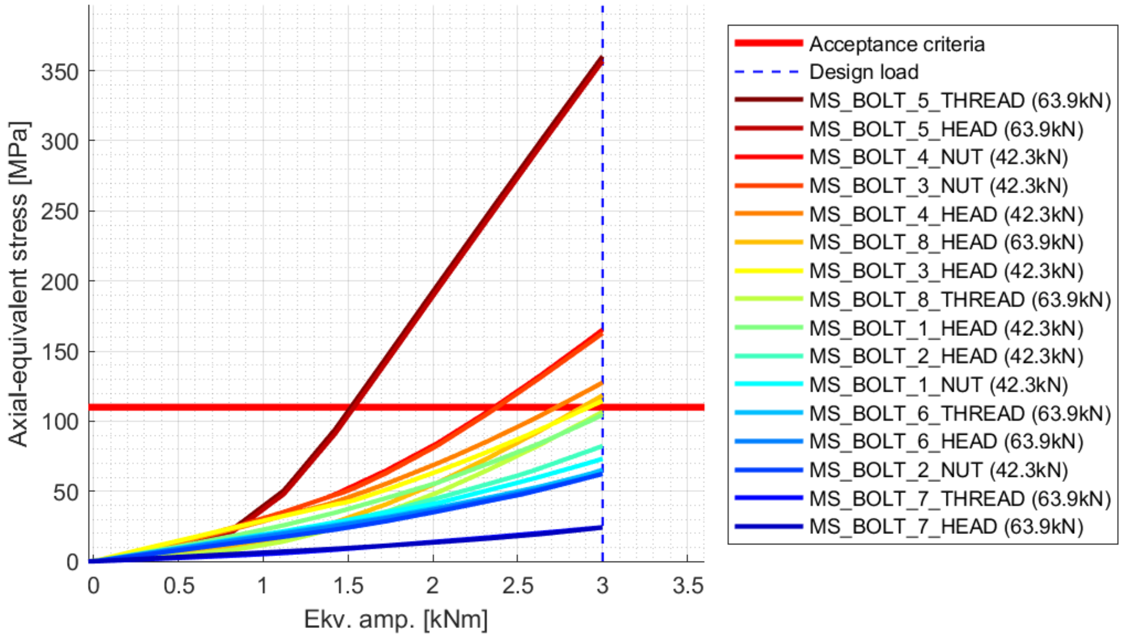

Figure 5: Plot of the axial equivalent stress for the bolts. The values in parentheses are the applied pretension forces.

Figure 6: Surface sections were the bending stresses are extracted for the bolt evaluation script. The section where the stresses for the head are evaluated is seen to the left and to the right for the bolt nut.

2.1.3 Bolt script

Most of the results obtained from the simulations used in the study are obtained from a script created by Scania, which is standard for evaluating bolts. The script extracts the bending stresses at 25 points around the circumference of the bolts from surface sections placed as seen in dark grey in Figure 6, the surface sections are placed 1 mm from the bolt head and the nut to capture the gradient of the bending stresses. [3]

The maximum bending stress at these points is then reduced with a factor used for the bending stresses. The axial equivalent stress is then calculated according to Eq. 1. The bending factor is used since it was concluded through several measurements that bolts exposed to pure bending have a fatigue life that is one third longer than bolts exposed to pure axial tension.[4] The reduced bending stresses are then added to the axial stress to obtain the axial equivalent stress at the bolt head and the bolt nut. This is done for every increment of the load in each step for the simulation. The axial equivalent stress is then plotted against the load for every increment as in Figure 5.

$$\sigma(t,\varphi) = \frac{P(t)}{\pi r2} + \frac{fb\big(\cos(\varphi)M1(t) + \sin(\varphi)M2(t)\big)4}{\pi r3} \qquad (1)$$

2.1.4 Bolted joints

There are many parameters and factors to consider when constructing and evaluating bolted joints. The purpose of a bolted joint is to clamp and fixate two or more parts. It is of great importance that the bolt/bolts have enough clamping force in order to prevent the clamped parts to slip. The stiffness relation between the bolts and the clamped parts is also an important factor to avoid that too much force goes through the bolts instead of the clamped parts, which otherwise could lead to failure in the bolts.

In Figure 7 [5], a $F - \delta$ diagram of a joint exposed to an external axial force, F_A, applied right under the bolt head and nut is presented. F_i is the pretension force, F_b, the force that the bolt is exposed to and F_c is the force that the clamped parts are exposed to. When the external load is increased, the clamped parts will feel a decrease in force and only the bolt will be exposed to the increase of the external force. The deformation in the clamped parts will therefore reduce while the deformation in the bolt will increase. The added force that the bolt is exposed to will be ΔF_b, while the clamped parts is exposed to the force ΔF_c. [5]

The new load that the bolt will experience when the outer loading is applied under the bolt is calculated as

$$F_b = F_i + F_A \frac{k_b}{k_b + k_c} \tag{2}$$

And the remaining force in the clamped parts, i.e. the remaining clamping force is calculated as

$$F_c = F_i - F_A \frac{k_c}{k_b + k_c} \tag{3}$$

From Equation (3) it is noted that when the external load becomes greater than F_i, the joint will be fully relieved and the bolted joint loses its function. In order to create an optimal bolted joint a higher stiffness of the clamped parts is preferred in comparison to the stiffness of the bolts.

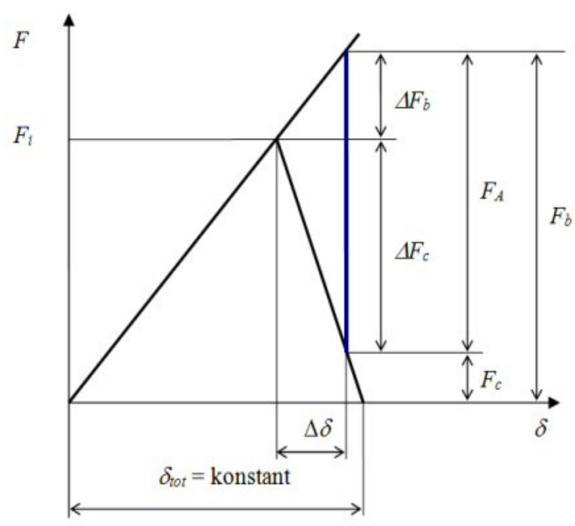

Figure 7: F-δ chart when the joint is exposed to an external loading

Friction and clamping force are important parameters for bolted joints experiencing shear forces. Friction is difficult to approximate and depends on many factors such as the painting or coating of the components, if there is oil on the surface, which type of materials are used in the joint and so on. In a bolted joint where shear forces are present, the joint is dependent on a clamping force that is sufficient enough for the friction force to overcome the shear forces created by external loading. When the external load overcomes the friction forces, the bolted joint will start to slip and bending stresses are introduced to the bolts. If slip is initiated at the bolt head and nut, self-loosening of the bolts can occur and the clamping force could therefore reduce.

Another factor that has a big impact on bolted joints is the clamping length of the bolts. A longer clamping length reduces the effects of loss in clamping force when embedment loss is present.

3 Method

In this chapter, the methods used for the rig test and the simulations are presented.

3.1 Rig test

The equipment and the different rig test executions is presented in this chapter

3.1.1 Equipment

A rig test has been conducted in order see how the behavior of the bolts develop at different load magnitudes. Measurements of the bending strain and the axial strain of the bolts were collected during the tests with strain gauges. The parts included in the rig test are listed in Table 3. The parts added compared to the setup used for the Wöhler test are presented as well. The frame used in the rig test is cut out from an extension frame member to represent the durability test and the boundary conditions as close as possible.

Alterations made to the beam and the beam brackets were to extend the radii of the holes from 7.75 mm to 9 mm. This was done in order to be able to feed through the cables from the strain gauges that were applied at the circumference of the bolts. More information of the strain gauges can be found in Chapter 3.2.

One of the beam brackets had threaded holes in the original design, the holes are seen in Figure 8. Since these threads were drilled away when the radii of the holes were extended, bolts with nuts have been used for the rig test instead.

Other equipment used in the rig is seen in Table 4. An alternating load is applied from a cylinder at the end of the beam as seen in Figure 9. The torque distance is calculated from the frame face with a distance of 0.71 m.

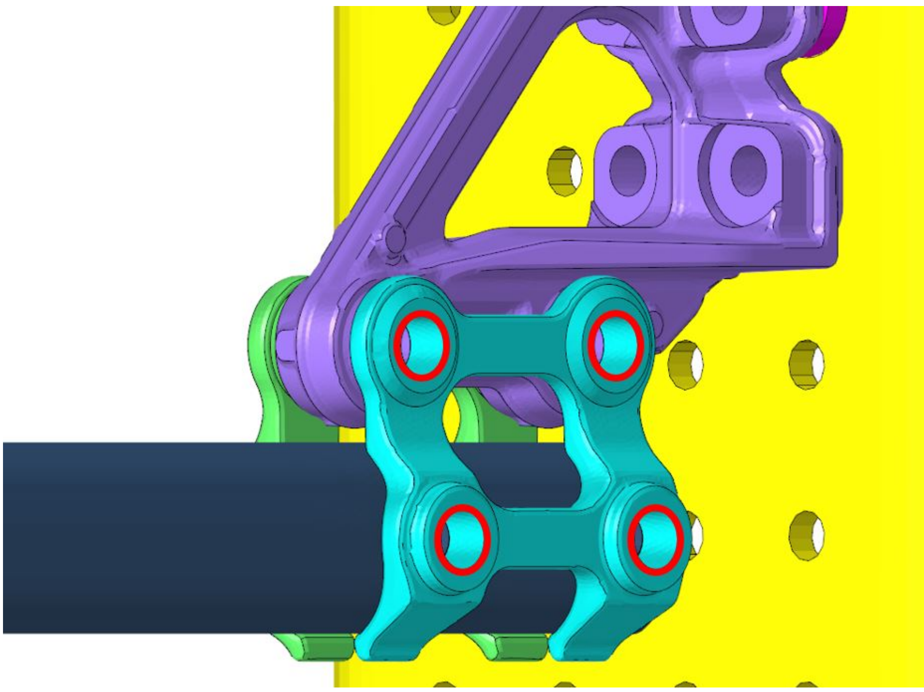

Figure 8: The threaded holes in the beam bracket are highlighted with red circles.

Table 3: Parts included in the rig test.

Component	Description	Material	Added part
Frame	Connected to the rig	Steel	
Frame bracket	Connected to the frame/beam bracket	Modular cast iron	
Beam bracket x 2	Connected to the frame bracket/beam	Steel	
Beam	Connected to the beam bracket and the cylinder	Aluminum	
Plain washers	15x26 height 2.5	Steel	X
Washers	15x34 height 8	Steel	
Hexagon head bolt	M14, 8.8	Steel	
Hexagon head bolt with flange	M14, 10.9	Steel	X
Hexagon nut with flange		Steel	X
Hexagon nut		Steel	X

Table 4: Other equipment used for the rig test.

Equipment	Description
Control system	MTS 407
Load indicator	±20 kN
Hydraulic cylinder	MTS 244.12
Measurement system	Dewetron

Figure 9: The cylinder to the left applies the load in global x-direction at the end of the beam.

3.1.2 Load series

Eight different load levels were applied to the mudguard bracket. The aim with the load series was to capture the loss of clamping forces due to embedment in the bolts and the clamped parts. It was also performed in order to evaluate the axial stresses together with the bending stresses of the bolts at higher loads. The torque amplitudes used for the load series are presented in Table 5. These were applied consecutively for approximately 30 cycles each.

3.1.3 100 000 cycle test

This test was performed to see how the bolts are affected during a quasi-static load case. The load amplitude was set to 1700 N to evaluate the bending and axial stresses for 100 000 cycles. With the torque distance of 0.71 m, the torque amplitude then becomes 1.9 kNm which was chosen according to the previous Wöhler test. An additional 65 000 cycles were performed to see if any of the beam bolts would fail.

3.2 Measurements

The bolts used in the rig test were equipped with strain gauges to collect data of the bolts behavior. Strain gauges were glued at the circumference of bolts 3-8 to capture the bending strains. In Figure 10, a schematic picture of the placement of the strain gauges is seen. With this placement, two half Wheatstone bridges are created. The bending strain around a specified axis can then be calculated through,

$$\sigma_{bi} = \frac{S_i - S_{i+2}}{2} \tag{4}$$

for i = 1,2, which are the local coordinates that the bolt bends around seen in Figure 10. All of the bolts were equipped with strain gauges glued in a drilled hole at the center of the bolts, in order to capture the axial strain.

The strain gauge cables were for the first bolts used in the testing fed through the bolt head, this protected the cables from being damaged during the pretension step. A different method to equip the strain gauges to the bolts was used for the second bolt batch. The cables of the strain gauges were now sticking out directly from the bolts circumference. To protect the cables a special washer was produced which can be seen in Figure 11. The washers also protected the gauges themselves since a gap was present between the bolts and the washer.

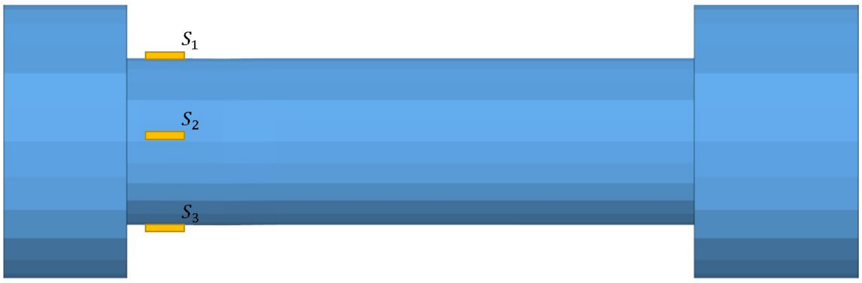

Figure 10: Schematic figure of the strain gauges applied on the bolts to create two half Wheatstone bridges.

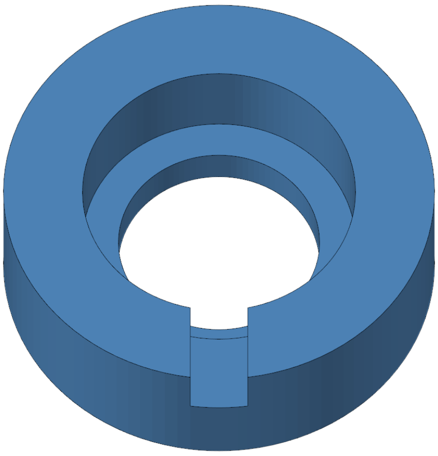

Figure 11: Modelled protection washer.

Table 5: Torque amplitudes applied for 30 cycles respectively.

Torque amplitudes [kNm]							
0.355	0.710	1.065	1.420	1.775	2.130	2.485	2.840

3.3 Simulation model

The different parts used to create the simulation model are presented in this chapter. ABAQUS is the solver being used while the geometry were meshed in HyperMesh.

3.3.1 Boundary conditions and the foundation of the simulation model

The foundation of the simulation model is seen in Figure 12. The parts included in the model are presented in Table 6 together with respective mesh and coloring of the parts in Figure 12.

Boundary conditions were set with fixation in all degrees of freedom at the highlighted areas seen in Figure 12. The load is applied with kinematic coupling at the far end of the beam. This results in a different torque distance compared to the rig test, the torque distance is obtained as 0.789m.

Differences between this simulation model and the previous one include the extended radii for bolt holes in the beam and the beam brackets to represent the rig test. Eight new holes have also been added to the frame as it was in the rig test.

Contact has been defined for the elements in areas were contact is present, which is seen in Figure 13.

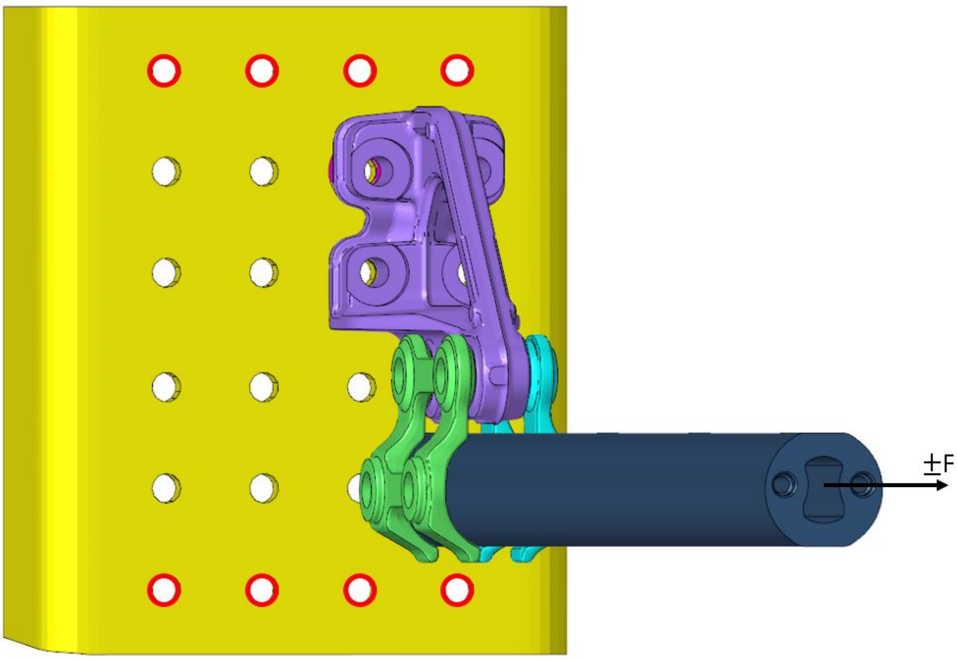

Figure 12: The foundation of the simulation model.

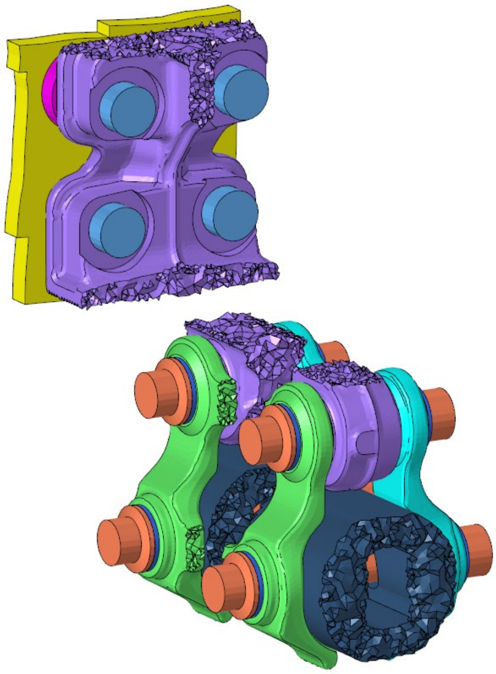

Figure 13: The areas were contact has been defined.

Table 6: Description of the parts included in the foundation of the simulation model

Component	Mesh	Color
Frame bracket	C3D10I	Purple
Beam bracket	C3D10I	Green/Turquoise
Beam	C3D10I	Dark blue
Frame	C3D8I	Yellow

3.3.2 Bolts

The bolts used in the simulations are created through a macro script. The script is developed by Scania. The radii used for the bolts body is the nominal radius and the mesh used is solid elements, C3D8I. The head of the bolt and the nuts are modelled with a circular geometry instead of hexagons to avoid stress concentrations.

The main difference between the simulation models are when it comes to the dimension of the bolts. Three different bolt lengths have been used for the simulations: one length to represent the beam bolts for when the threaded beam bracket was used, one for the unthreaded case where nuts were used for the beam bolts, and one bolt length for when the protection washers were added to the beam bolts. The different clamping lengths are presented in Table 7. Furthermore, hexagon nuts were used for one evaluation and flange nuts for a second evaluation. For the case with threaded beam bracket, the nuts has been removed for the beam bolts, and a tie has been set between the bolt end and the beam bracket, as seen in Figure 17. Tie is an ABAQUS specific term which means that the translational and rotational motion are equal for a pair of surfaces and their nodes [6].

Strain gauges were modelled in order to compare the results obtained from strain gauges in the physical test and to evaluate the reliability of the extracted stresses from the bolt script, where the maximum stresses are obtained. The strain gauges have been modelled with one dimensional T3D2, rod elements, as seen in Figure 16. They are placed 2 mm from the bolt head and have a length of 3 mm.

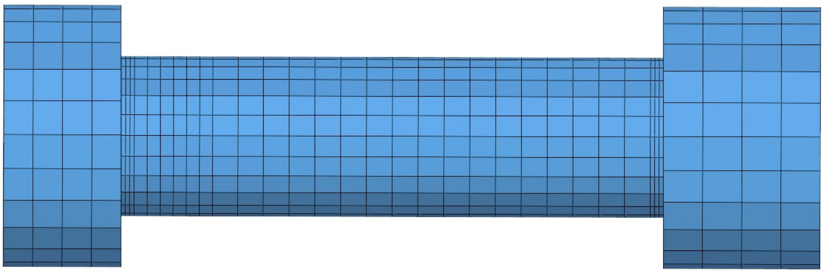

Figure 14: Modelled bolt for representation of a hexagon nut to the left, the hexagon nut is modelled with a circular geometry in order to avoid stress concentrations.

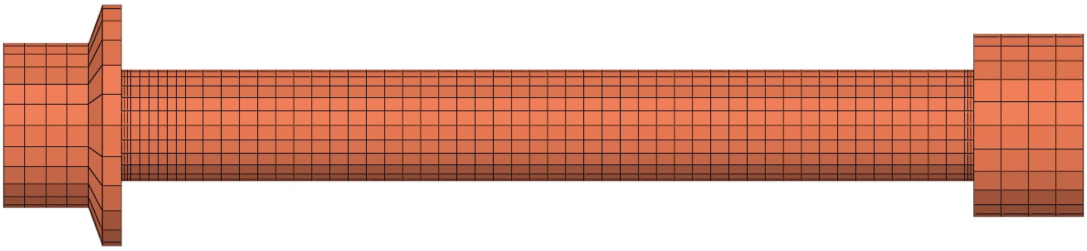

Figure 15: Modeled bolt for representation of a flange nut to the left.

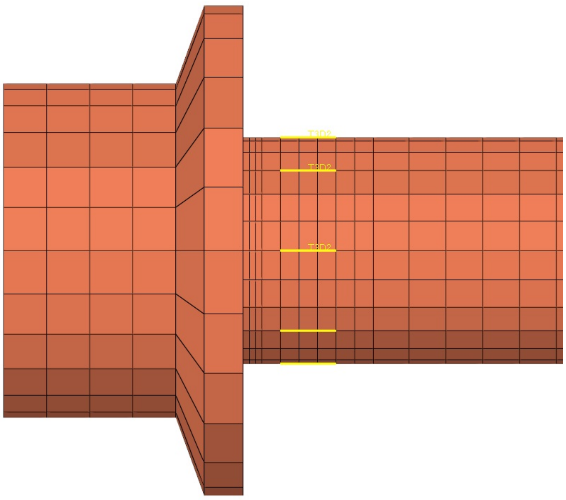

Figure 16: The modelled strain gauges are seen in yellow on the surface of the bolt body.

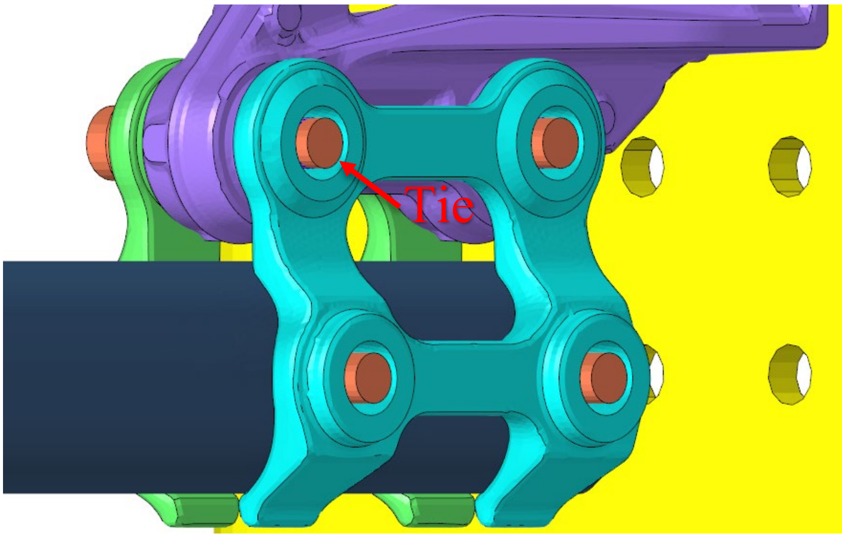

Figure 17: Tie is set at the end of the four beam bolts to represent the threaded beam bracket.

Table 7: The different clamping lengths used for the bolts.

Bolts	Threaded bracket [mm]	Unthreaded bracket [mm]	Unthreaded bracket, added protection washers [mm]
1 and 2	41.5	41.5	41.5
3 and 4	33.5	33.5	43.5
5 and 6	44.5	60.2	66.2
7 and 8	76.0	93.2	99.2

3.4 Simulations

Three main parameters have been evaluated in the study, friction, clamping length and pretension force.

The clamping length of the bolts have been evaluated, to investigate the differences of the results obtained for the different bolt lengths used in the rig test. The different clamping lengths that have been evaluated can be seen in Table 7.

Different pretension forces have been evaluated according to clamping forces present during the rig test. A total of three different pretension combinations has been evaluated for the frame and beam bolts. The pretension forces are presented in Table 8. Combination 1 were evaluated in order to match the pretension forces used for the measurements obtained when the external load where applied. For combination 2 are the beam bolts pretension forces increased, this to match the measured pretension force directly after they were tightened and no external load has been applied. Combination 3 is with a pretension force for the bolts used in simulations according to Scania standards for normal torque and torque/angle respectively when an estimated 10% reduction of clamping force due to embedment loss is taken into account.

The friction has been investigated to find out how the behavior of the bending stresses changes with different coefficients, and to find a better correlation to the physical test result. The coefficients evaluated are $\mu = 0.15$ according to standards, $\mu = 0.20$, $\mu = 0.25$ and $\mu = 0.30$.

The load is applied with two different methods. For the first case the load is applied in two independent "steps" according to the standard method when the bolt evaluation script is used. The pretension step is the first step in the input file, followed by one step for the positive load direction, and one step for the negative load direction, independent of each other. A "step" is a term used in ABAQUS which means that a specific procedure is being performed during the step in the analysis.

When the standard method was used, the hysteresis that appears due to slip is lost (which will be discussed further in Chapter 3.5). Because of this, analyses have been performed where the load steps are applied consecutively to each other, which creates a cyclic alternating torque more similar to the obtained measurements in the physicals test.

3.5 Correlation

In order to improve the correlation between the measurements and the simulations comparisons has been set out with a couple of different methods throughout the study. Initial was the maximum value of the bending and axial stress amplitudes the main method to compare the measurements to the simulation results when the load were applied as for the first case, since the behavior of stresses in the plots were difficult to compare. Once the load were applied according to the second method in consecutive steps, the stress plots became more similar. The total behavior of the stresses during loading could therefore be compared with the plots of the bolts behavior from measurements and simulations in order to detect differences more than just a discrepancy in the stress amplitudes.

The axial equivalent stress will not be compared between the measurements of the bolts and the simulation results obtained by the bolt evaluation script. The stresses are extracted from the bolts heads and nuts in the simulation model in such a way that a comparison would not be fair.

Table 8: The combination of pretension forces evaluated in simulations.

Bolt set	**Clamping forces [kN]**		
	Combination 1	Combination 2	Combination 3
1-4	22.3	22.3	42.3
5-8	72.7	82.7	92.7

4 Results

In this section the results from the rig test and the simulations are presented.

4.1 Rig test

4.1.1 Clamping forces

Measurements of the clamping forces obtained directly after the bolts were tightened can be seen in Table 9. According to [3], bolts 1-4 should have an initial clamping force of 47 kN before embedment loss is taken into account. Since the data is collected during the pretension of the bolts, no embedment should have occurred yet. Therefore, this value is used instead of the pretension force used in the simulation where a 10 % reduction of the clamping force due to embedment loss is accounted for. The pretension force for bolt 5-8 is set to 103 kN according to [3].

The initial clamping forces before two load series of eight load levels are compared to the clamping forces after the two load series were conducted in Table 10.

When compared, it is seen that there is significant loss of clamping forces for the frame bolts with a maximum loss of 28 % for bolt 3. For the beam bolts the maximum loss of clamping force was 1 %.

The measured clamping forces before and after 10 000 cycles are presented in Table 11. The percentage of the clamping force loss is significant for all the frame bolts here as well. Bolt 1 has a maximum loss of 100 %, although without failure in the bolt.

The beam bolts do not experience any significant loss of clamping force after 10 000 cycles. This is also the case after 165 000 cycles where bolt 6 had a maximum loss of clamping force of 3 %.

Table 9: Clamping forces for the bolts right after pretension together with the discrepancy of the expected pretension force.

Bolt	Pretension force [kN]	Discrepancy
1	54	+15 %
2	58	+23 %
3	40	-15 %
4	42	-10 %
5	110	+7 %
6	90	-13 %
7	84	-18 %
8	92	-10 %

Table 10: The difference of the bolts clamping forces before two load series with eight load levels respectively were performed, together with the clamping force after two load series were performed.

Bolt	Clamping force before the load series [kN]	Clamping force after two load series [kN]	Loss in clamping force
1	44	32	27 %
2	43	34	22 %
3	24	18	28 %
4	31	22	27 %

Table 11: The clamping forces before test were started, together with the clamping forces after 10 000 cycles and the discrepancy between them.

Bolt	Clamping force before the test	Clamping force after 10 000 cycles	Loss in clamping force
1	31	0	100 %
2	33	19	42 %
3	17	12	29 %
4	22	17	23 %
5	73	72	1 %
6	69	69	0 %
7	82	81	1 %
8	83	83	0 %

4.1.2 Wear and slip

The wear after more than 165 000 cycles of the frame and the frame bracket is seen in Figure 18. Significant signs of slip can however be seen in the frame bracket. The wear that arises at bolt 5 is seen at the bottom picture in Figure 18. This shows that slip is most certainly appearing between the frame bracket and the beam bracket.

Figure 18: The wear of clamped components. The top figures show the wear of the frame to the left and the back of the frame bracket where the frame bolts are located to the right. The bottom picture shows the wear of the frame bracket, where bolt 5 was located to the right and bolt 6 to the left.

The influence of the slip at bolt 5 can also be noticed in the bending stresses for when the applied torque amplitude is 2.84 kNm, seen in Figure 19 and Figure 20. The fact that a hysteresis is present implies that slip is initiated where the gradient of the curve increases. The slip is initiated when the torque is relieved from a negative direction and exceeds approximately a positive torque of 1 kNm for bending around the y-axis. Once the torque is relieved from a positive direction, the slip is initiated at 0 kNm as the force becomes negative.

The amplitude of the bending stress around the y-axis is 124 MPa and the bending stress around the z-axis is 109 MPa. The axial stress amplitude for bolt 5 seen in Figure 21 is calculated to 10 MPa.

The bending stresses for bolt 4 are seen in Figure 22 and Figure 23. The influence of the slip is not as significant as for bolt 5 when looking at hysteresis of the graph. The amplitude of the bending stress around the x-axis is approximately 144 MPa and the stress around the z-axis is 22 MPa. The axial stress for bolt 4 is plotted in Figure 24 with an amplitude of 75 MPa.

The bending stresses for bolt 3 and bolts 6-8 for a torque amplitude of 2.84 kNm can be found in the Appendix.

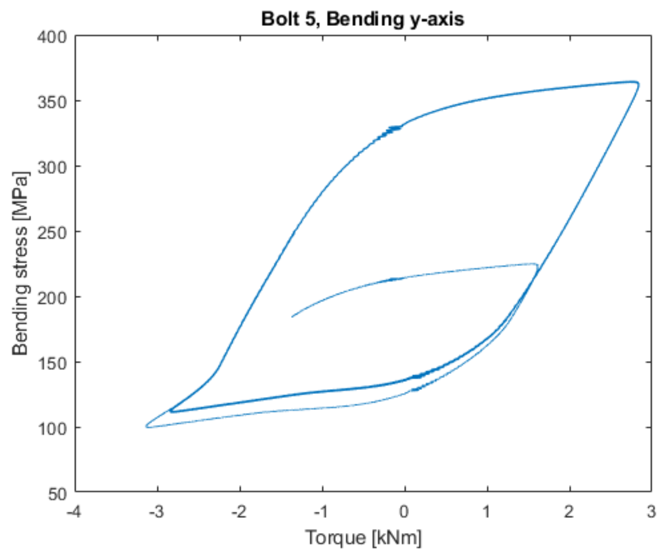

Figure 19: The bending stress around the y-axis for bolt 5.

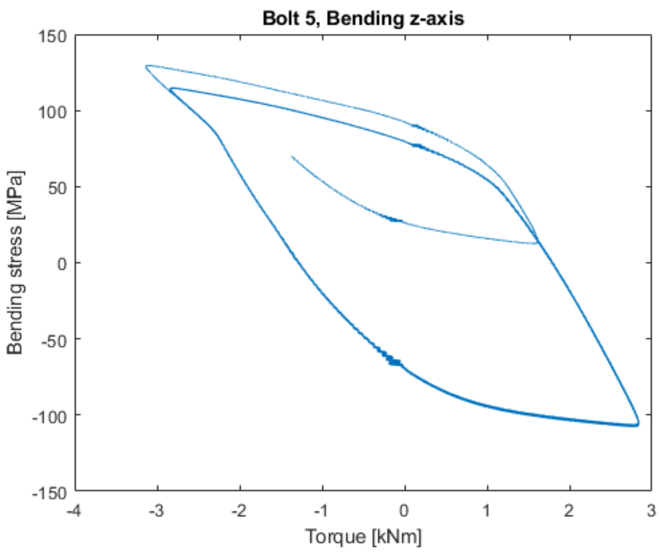

Figure 20: The bending stress around the z-axis for bolt 5.

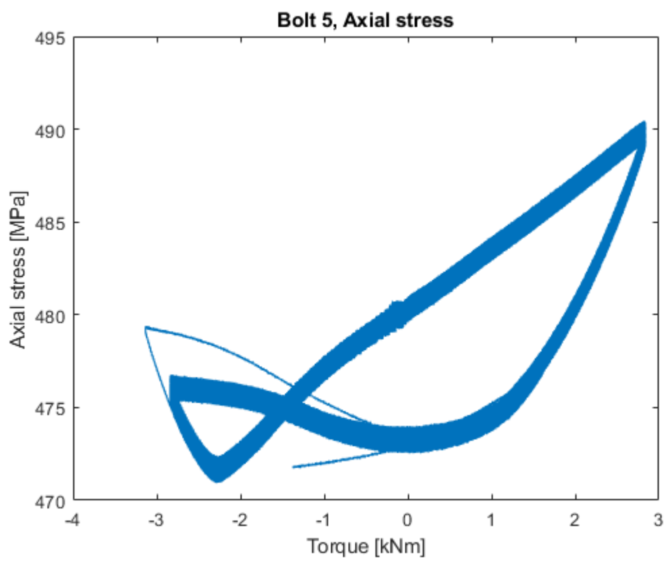

Figure 21: The axial stress for bolt 5.

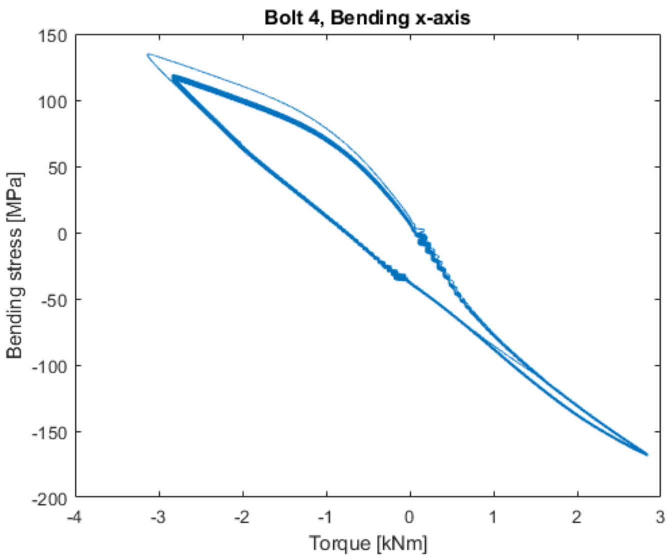

Figure 22: The bending stress at the x-axis for bolt 4.

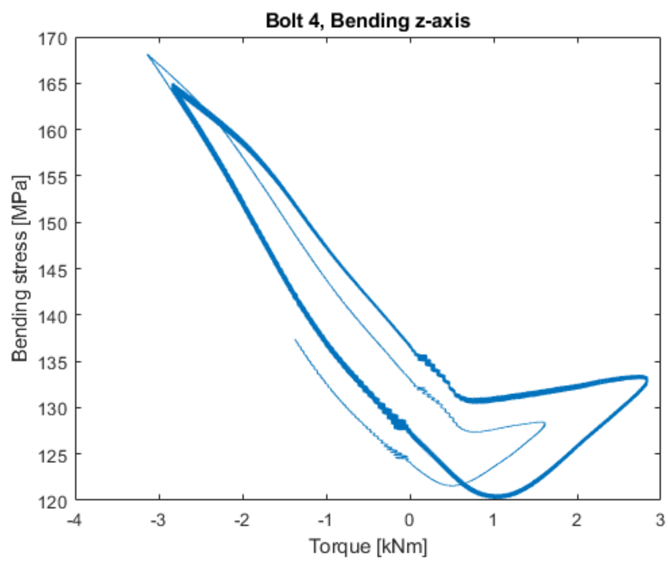

Figure 23: The bending stress at the z-axis for bolt 4.

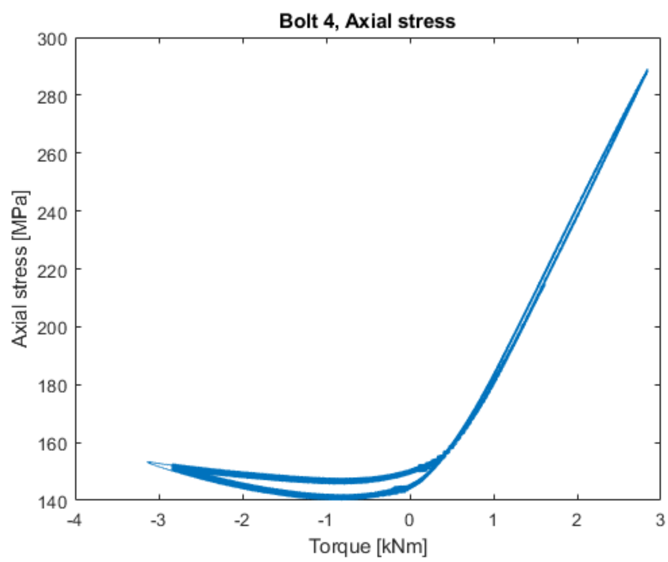

Figure 24: The axial stress for bolt 4.

4.1.3 Equivalent axial stress

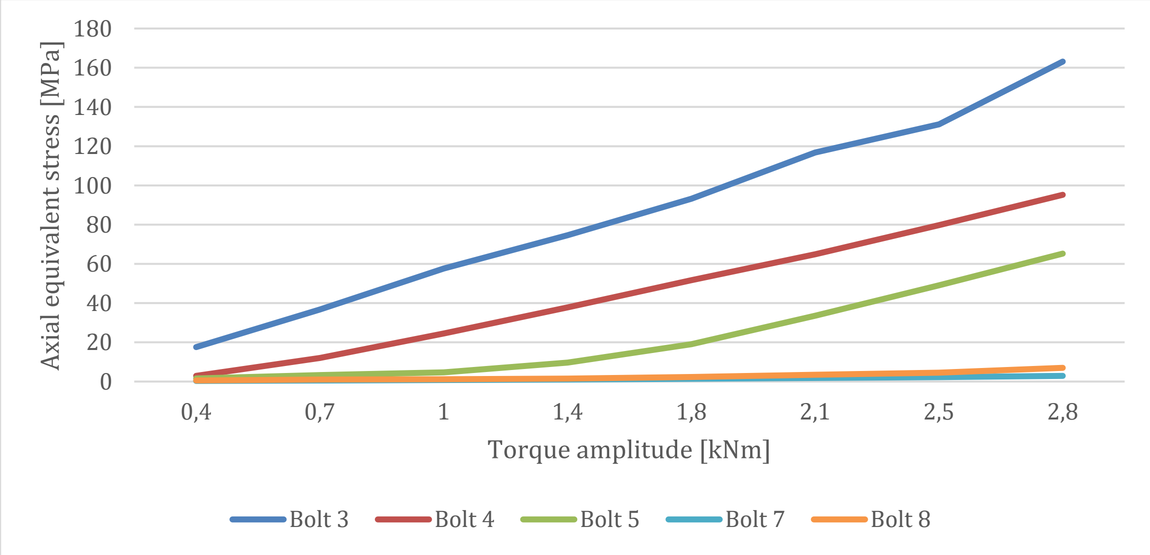

Figure 25: The axial equivalent stress for bolts 3-8 calculated for eight consecutive load levels.

The axial equivalent load has been calculated from the measurement data for the load series, the result is presented in Figure 25. The results show that bolt 3 is the only bolt that exceeds the acceptance criteria of 110 MPa and therefore would not be expected to withstand 100 000 cycles at a torque amplitude of 1.9 kNm. Bolt 4, which was critical in the first Wöhler test, has an axial equivalent stress below the acceptance criteria. The nonlinear behavior of bolt 5 indicates that slip is initiated between a torque amplitude of 1.1 kNm and 1.4 kNm. Bolts 6-8 all show low levels of stress and no significant signs of slip at higher load levels. Bolts 3 and 4 do not show any significant sign of slip occurring.

4.2 Simulations

4.2.1 Clamping length

When the clamping length of the bolts used in the new model is the same as the clamping length of the model used in the background, the results seen in Figure 26 show that there are no significant differences between the predictions for the bolts. This implies that there are no differences in the two models above the clamping length of the bolts.

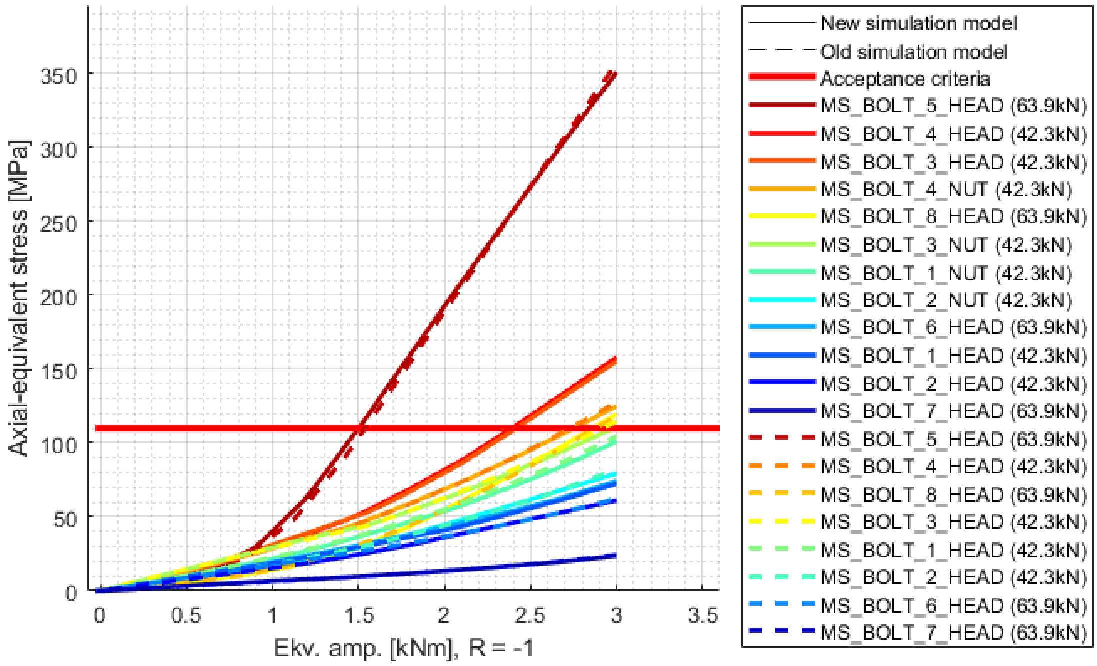

Figure 26: Evaluation that no significant differences is found between the bolts, according to the bolt evaluation script for the two simulation models.

4.2.2 Pretension forces, friction coefficient and applied load according to standards

Compared to the simulation results presented in the background in Chapter 2.1.2, an increased pretension force is used for the beam bolts, the pretension force used is now according to standards. The results of the analysis when the standard pretension forces and the friction coefficient is used can be seen in Figure 27. The prediction of the 100 000-cycle load for bolt 4 is 2.39 kNm and 2.18 kNm for bolt 5.

The results obtained from the bolt script show that there is significant slip occurring at bolt 5 when the torque reaches a magnitude of 0.9 kNm. It is seen that a high amount of slip is already initiated at a negative torque of 0.9 kNm as seen for the accumulated incremental relative motion (cslip) in Figure 28. The maximum amount of slip is obtained at bolt 5 when a negative torque of 3 kNm is applied, the cslip is then approximately 220 µm.

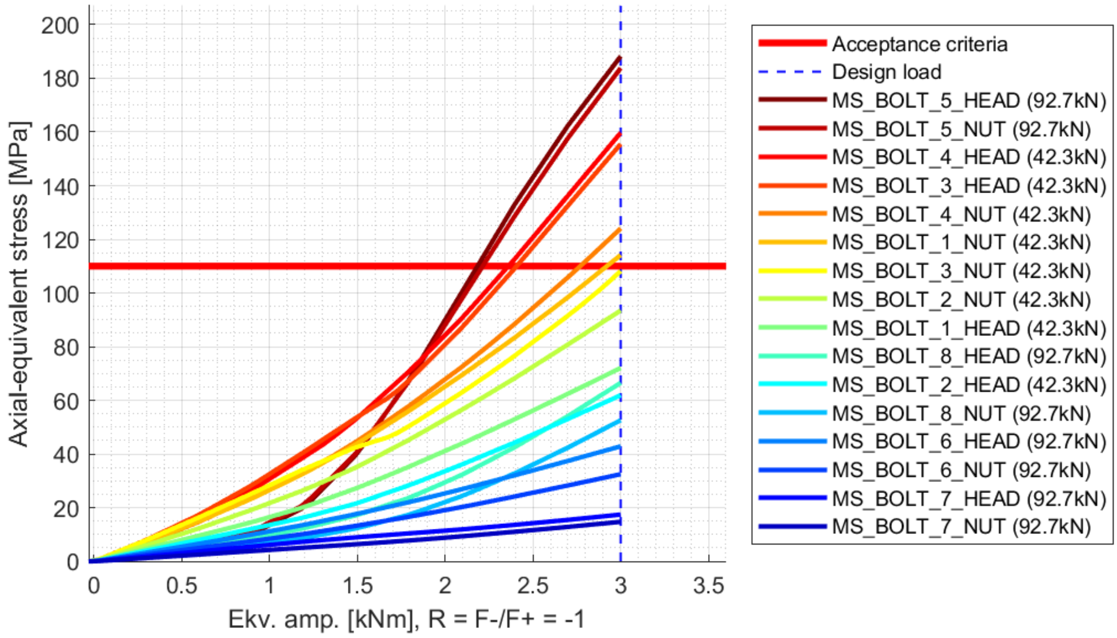

Figure 27: The axial equivalent stress for the bolts when the standard pretension force and friction coefficient is used.

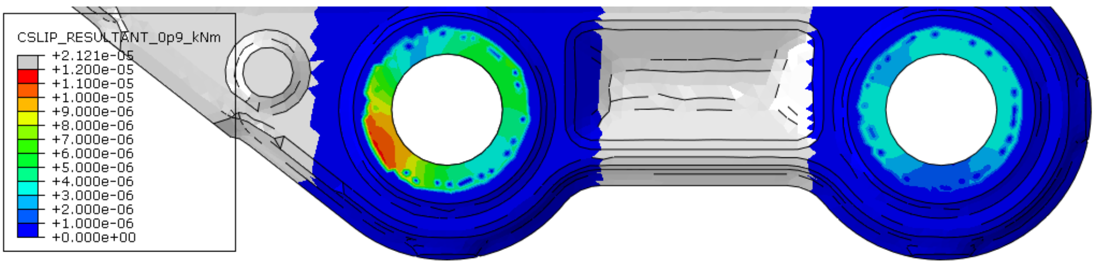

Figure 28: The cslip resultant between the frame bracket and the beam bracket at bolt 5 and 6 for when a torque of 0.9 kNm is applied in negative x-direction. NB: The scale is set from 0 to $1.2 \cdot 10^{-5}$m

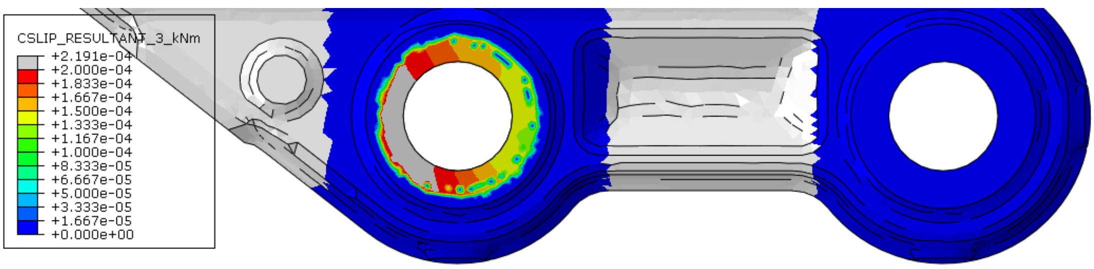

Figure 29: The cslip resultant between the frame bracket and the beam bracket at bolt 5 and 6 for when a torque of 3 kNm is applied in negative x-direction. NB: The scale is set from 0 to $2.0 \cdot 10^{-4}$m

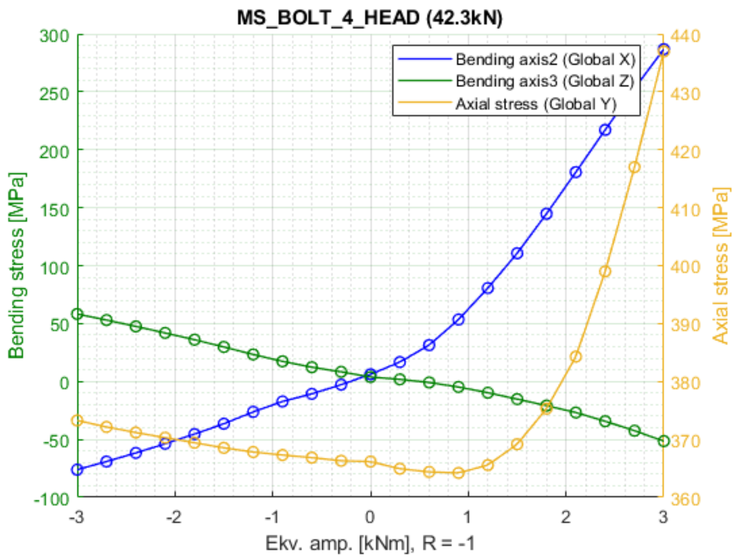

Figure 30: The axial stress together with the maximum bending stress for bolt 4, the pretension force is shown in the heading.

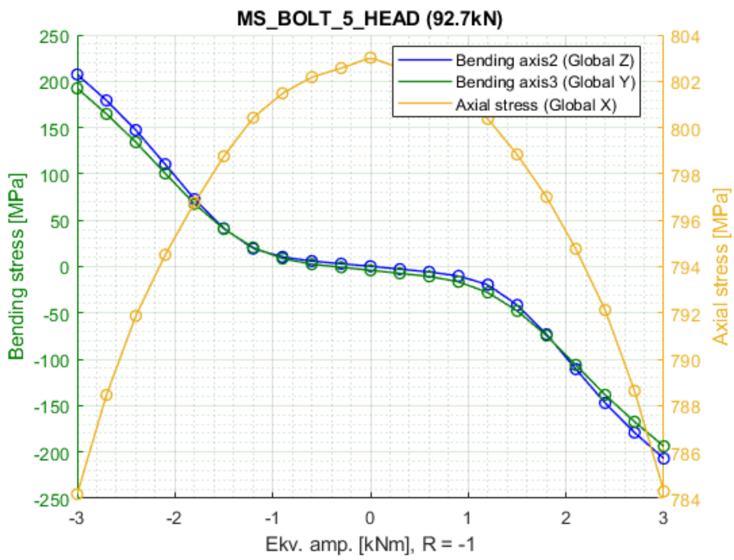

Figure 31: The axial stress together with the maximum bending stresses for bolt 5, the pretension force is shown in the heading.

The maximum bending stress and the axial stress obtained at the surface sections at the bolt head for bolt 4 and 5 are plotted in Figure 30 and Figure 31. The bending stress amplitude around the x-axis for bolt 4 is 182 MPa and 55 MPa around the z-axis, while the axial stress amplitude is 10 MPa. It is seen once again that the nonlinear behavior for bolt 5 starts at a torque amplitude of ± 0.9 kNm, and with a stress amplitude of 207 MPa for both the bending around the y- and z-axis, while the axial stress amplitude is at 37 MPa.

4.2.3 Load applied in consecutive steps

In Figure 32 and Figure 33, the bending stresses of bolt 5 are plotted for when the load steps have been applied in consecutive steps. The stresses are extracted from the rod elements that represent the strain gauges in the simulation model. During the first quarter cycle it is noted that slip is initiated at a torque magnitude of 0.9 kNm for the bending around the y-axis. However, the slip initiation starts once again when the load is ramped down to 1.1 kNm. Approximately the same behavior is noted for the bending around the z-axis although with an opposite sign in bending stresses. The hysteresis is stable after approximately half a load cycle.

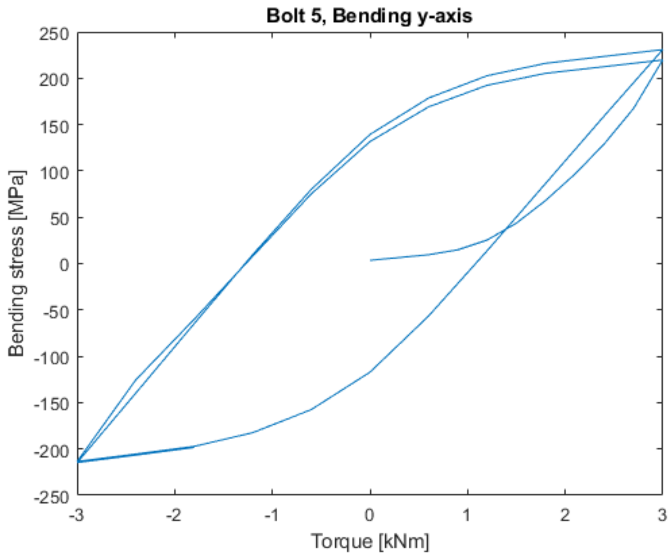

Figure 32: The bending stresses extracted from the modeled strain gauges for bolt 5 around the y-axis.

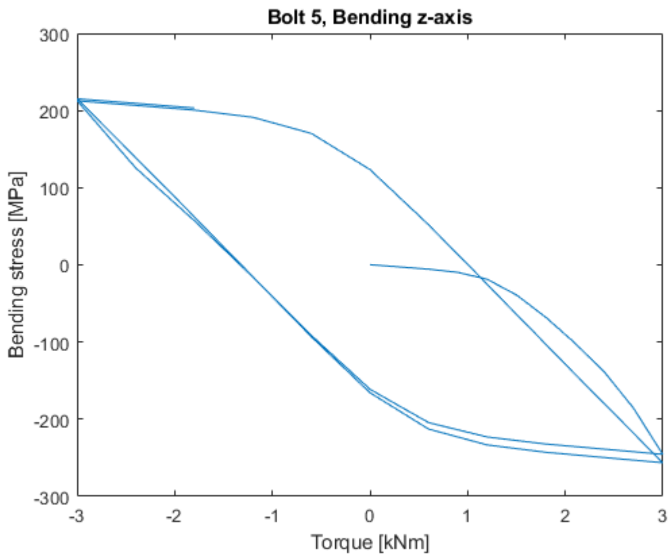

Figure 33: The bending stresses extracted from the modeled strain gauges for bolt 5 around the z-axis.

4.2.4 Pretension force

The results for when the applied pretension force of the bolts has been reduced to the values seen in the second column in Table 8 are presented in Figure 34. The 100 000 cycle loads for the bolts are obtained by the bolt evaluation script. The effects are as expected and the prediction for bolt 4 has now a decreased 100 000-cycle load of 1.83 kNm which is a decrease of 23 %. The torque that bolt 5 can withstand for 100 000 cycles is decreased to 1.83 kNm.

The bending stresses for bolt 4 and bolt 5 together with the axial stress are seen in Figure 35 and Figure 36. The plots show that the critical bending stress around the x-axis for bolt 4 has increased to an amplitude of 211 MPa and the axial stress amplitude has increased to 78 MPa. The bending stresses for bolt 5 has now increased to an amplitude of 253 around the y-axis and to 284 MPa around the z-axis and the axial stress amplitude is now 4 MPa.

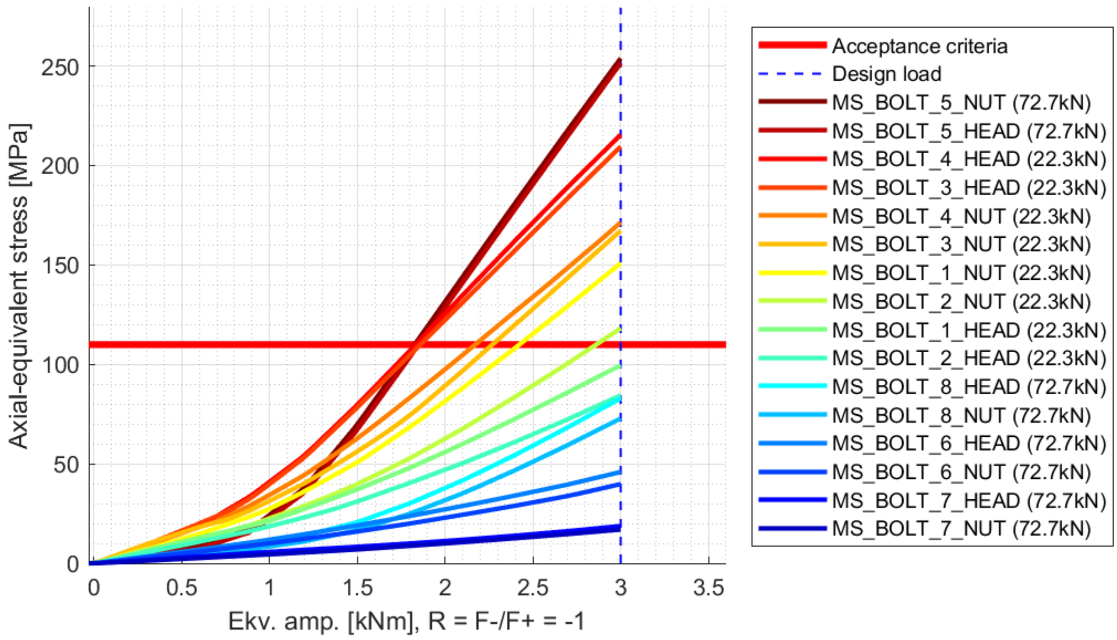

Figure 34: The axial equivalent stress for when the clamping force of the bolts has been reduced according to the physical test results.

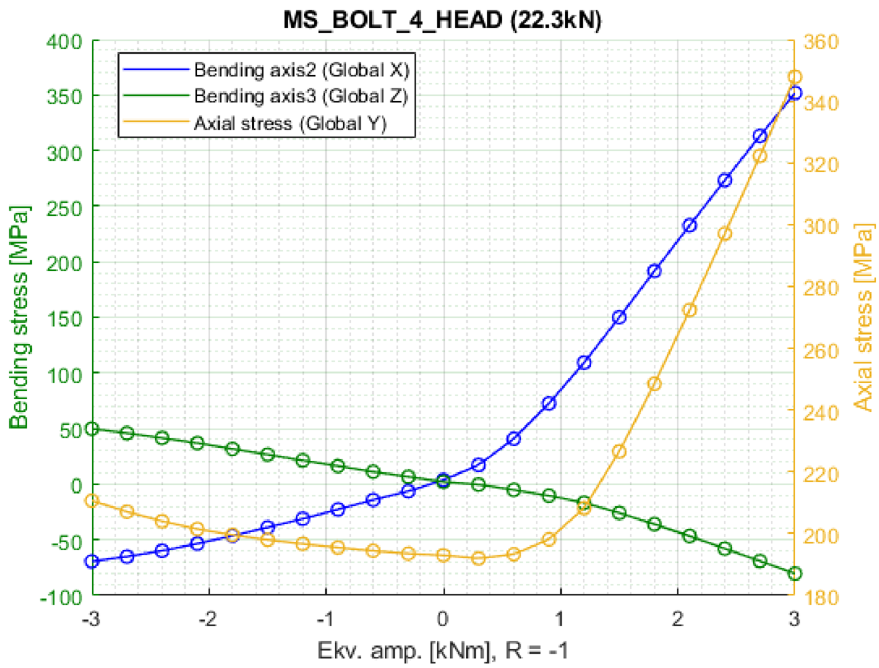

Figure 35: The bending and axial stresses obtained by the bolt evaluation script for bolt 4.

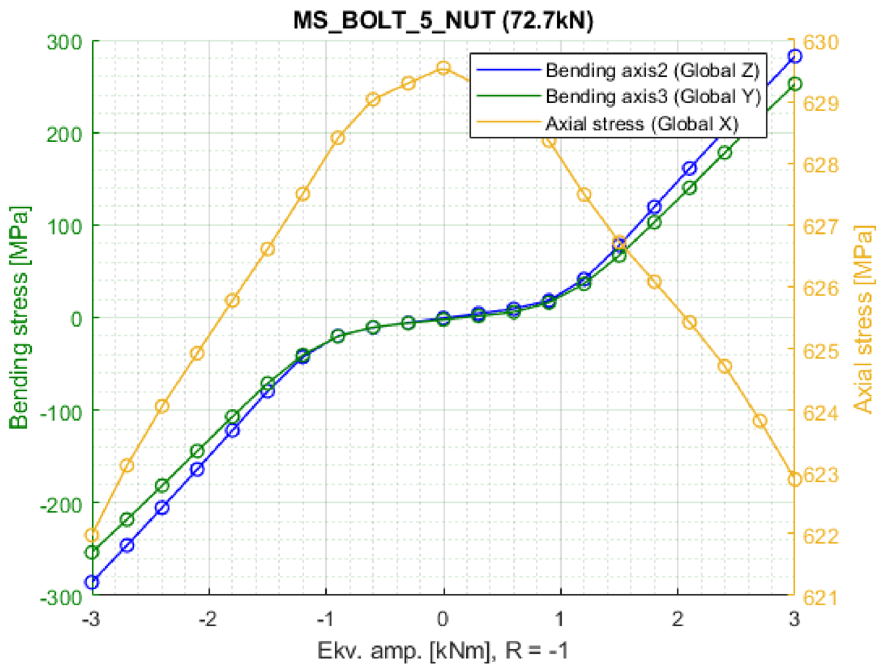

Figure 36: The bending and axial stresses obtained by the bolt evaluation script for bolt 5.

The behavior of bolt 5 for when the external load is applied in consecutive steps is seen in Figure 37 and Figure 38. The stress amplitude obtained from the simulation is for the bending around the y-axis 256 MPa and 267 MPa for the z-axis.

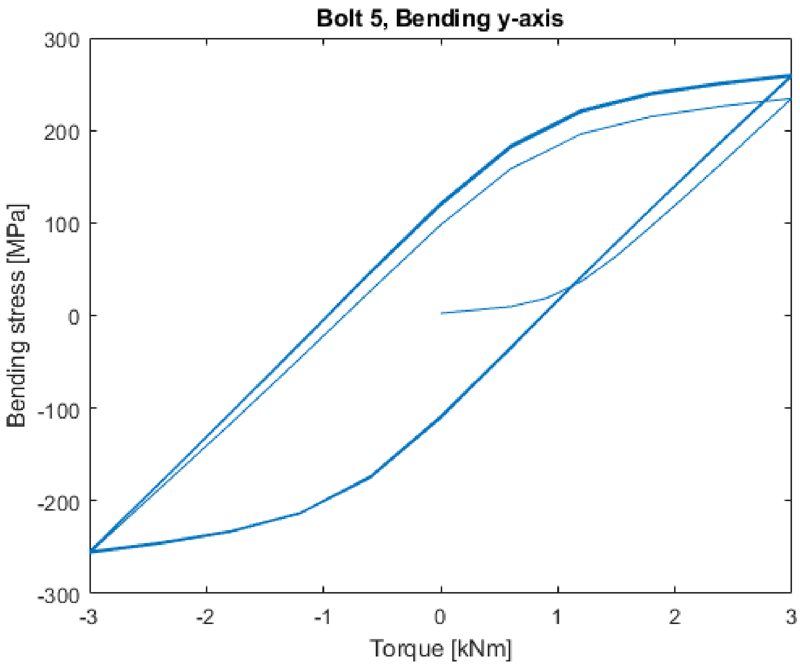

Figure 37: Bending stresses around the y-axis obtained for simulation with consecutive load steps for bolt 5 when the pretension force is set to 72.7 kN.

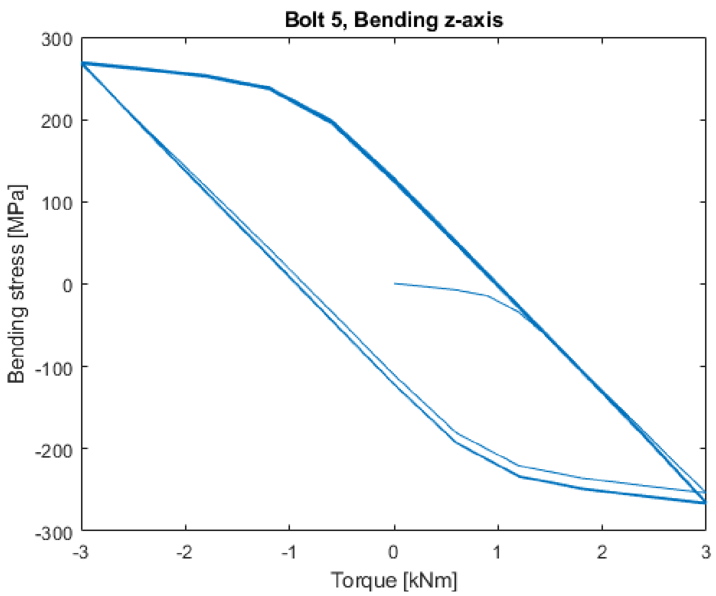

Figure 38: Bending stresses around the z-axis obtained for simulation with consecutive load steps for bolt 5 when the pretension force is set to 72.7 kN.

Another investigation has been done for when the applied pretension force of the beam bolts are according to the measured force right after the bolts were tightened, seen in Table 9. The new 100 000-cycle loads are seen in Figure 39. The 100 000-cycle load for bolt 5 is now 2.00 kNm while bolt 4 is unchanged.

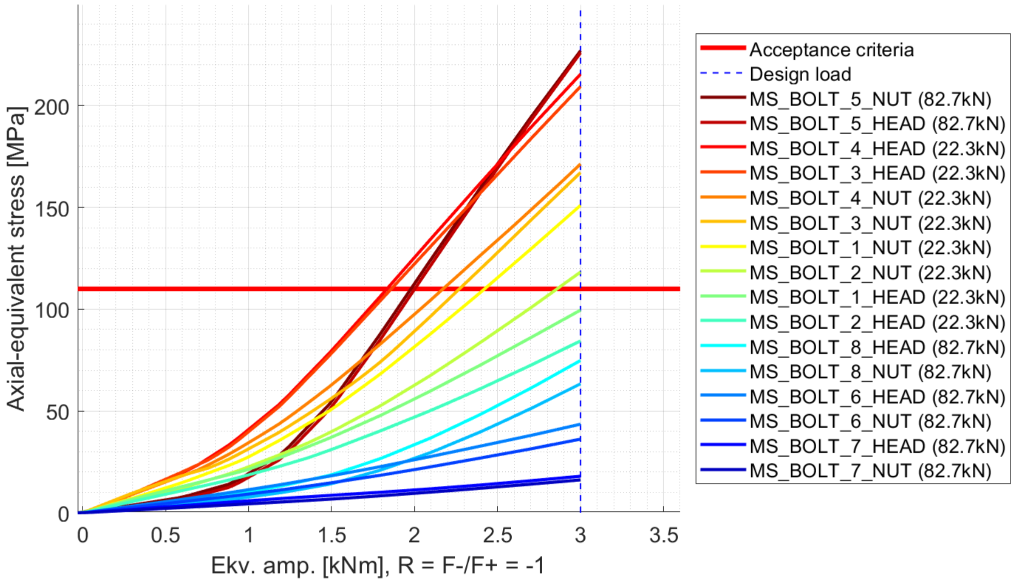

Figure 39: The axial equivalent stress for when the clamping forces of the beam bolts are according to initial measured pretension.

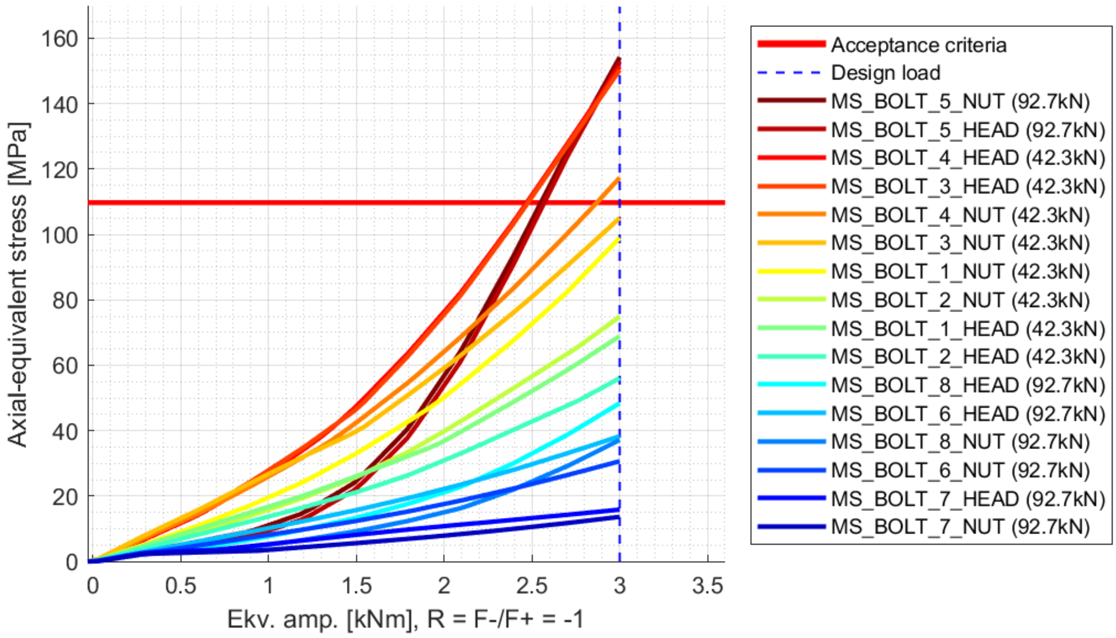

Figure 40: The axial equivalent stress of the bolts with a friction coefficient of 0.2.

4.2.5 Friction

The simulation results in Figure 40 where a friction coefficient of 0.2 is used show that the 100 000-cycle load has been increased for all the bolts. The bolt that has been most affected by the higher friction coefficient is bolt 5. The 100 000-cycle load for bolt 5 has been increased to 2.57 kNm, compared to 2.18 kNm when the friction coefficient was set to 0.15, which is an improvement of 18 %. Bolt 4 that failed during the first Wöhler test, now has a 100 000-cycle load that has been increased by 3 %.

In Figure 41 and Figure 42, the bending stresses and the axial stress for bolt 4 and 5 are presented respectively. The bending stress amplitude around the x-axis for bolt 4 is 170

MPa and 61 MPa around the z-axis and the axial stress amplitude is calculated to 35 MPa. Bolt 5 shows a bending stress amplitude of 158 MPa around the y- and z-axes. The axial stress amplitude is as seen 5 MPa. It is also noted that there is a jump for the axial stress for bolt 5, this is a consequence of the friction coefficient being increased in the step after the pretension step.

The bending stresses extracted from the modelled strain gauges for bolt 5 when the cyclic simulation is performed with a friction coefficient of 0.2 are seen in Figure 43 and Figure 44. The amplitude of the bending stress around the y-axis has been reduced to a magnitude of 170 MPa, while it has been reduced to 182 MPa for the bending around the z-axis. The slip is now initiated when the torque is relieved to a magnitude of approximately 0.5 kNm for the bending around the z-axis.

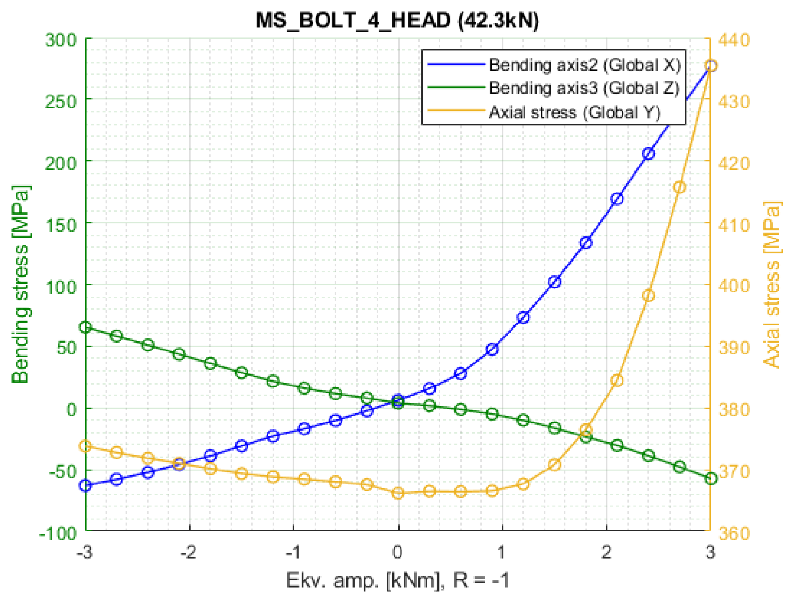

Figure 41: Bending stresses obtained by the bolt evaluation script for bolt 4 for when the friction coefficient is set to 0.2.

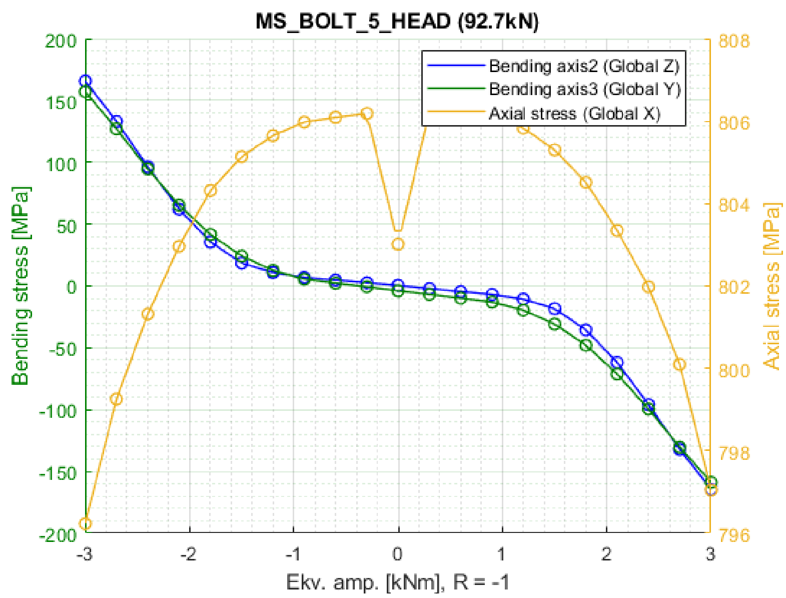

Figure 42: Bending stresses obtained by the bolt evaluation script for bolt 5 for when the friction coefficient is set to 0.2.

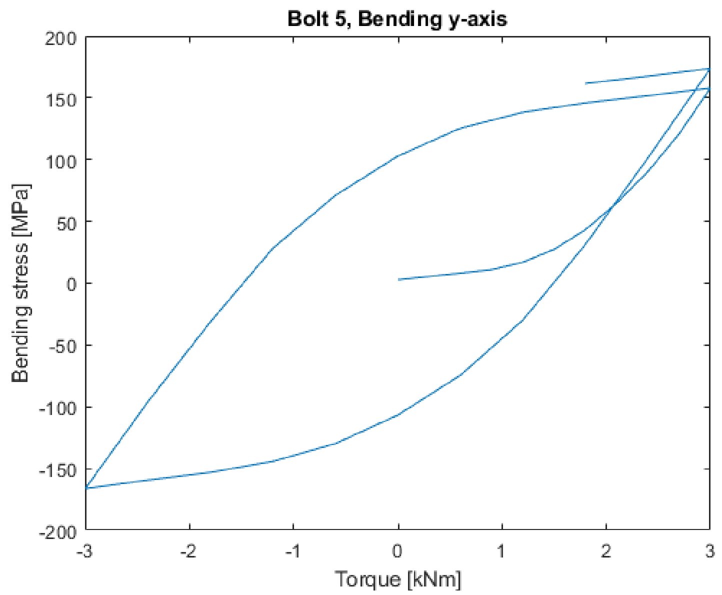

Figure 43: The bending stresses obtained by the modeled strain gauges for bolt 5 with a new friction coefficient of 0.2.

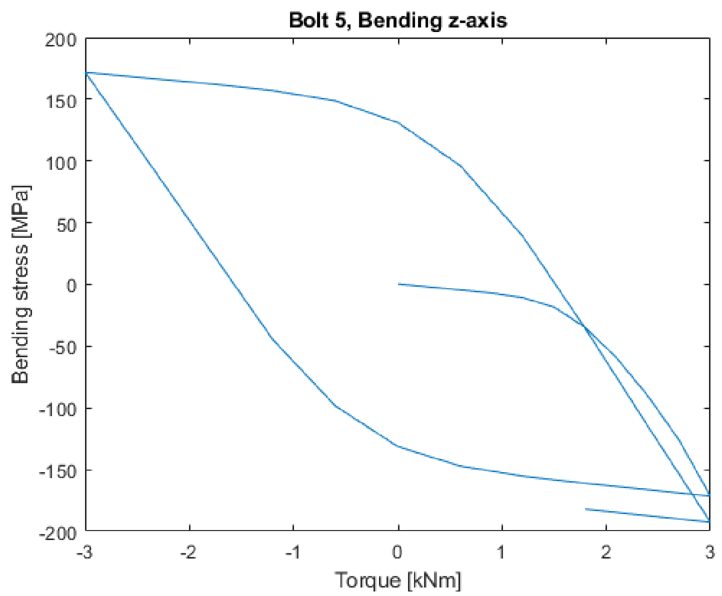

Figure 44: The bending stresses obtained by the modeled strain gauges for bolt 5 with a new friction coefficient of 0.2.

A simulation was performed with the friction coefficient set to 0.25. It can be seen in Figure 45 that the 100 000-cycle load of all the bolts has been increased. The effect is, as expected, most significant for bolt 5 which has a new load for the acceptance criteria at 2.88 kNm. The 100 000 cycle load for bolt 4 has increased to 2.54 kNm.

The bending stresses for bolt 5 obtained by the bolt evaluation script are seen in Figure 46. The stress amplitude is calculated to 125 MPa for the bending around both the z- and y-axes.

The plot of the bending stresses for bolt 5 when the friction coefficient is set to 0.25 is presented in Figure 48. The stress amplitudes obtained are similar to the stresses obtained by the bolt evaluation script with a magnitude of 128 MPa.

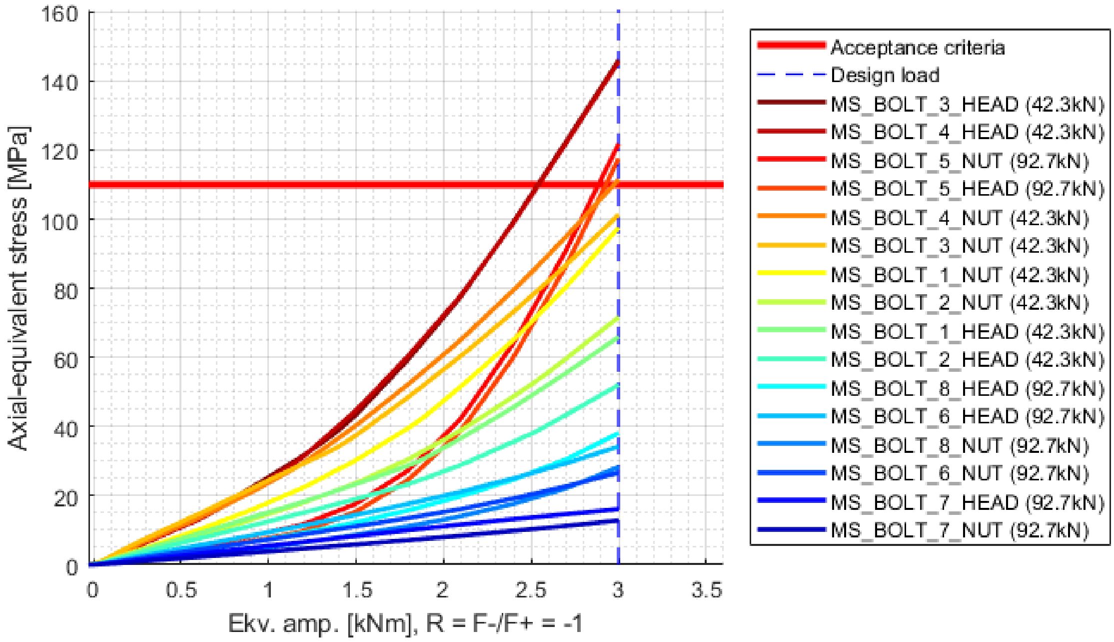

Figure 45: The axial equivalent stress of the bolts with a friction coefficient of 0.25.

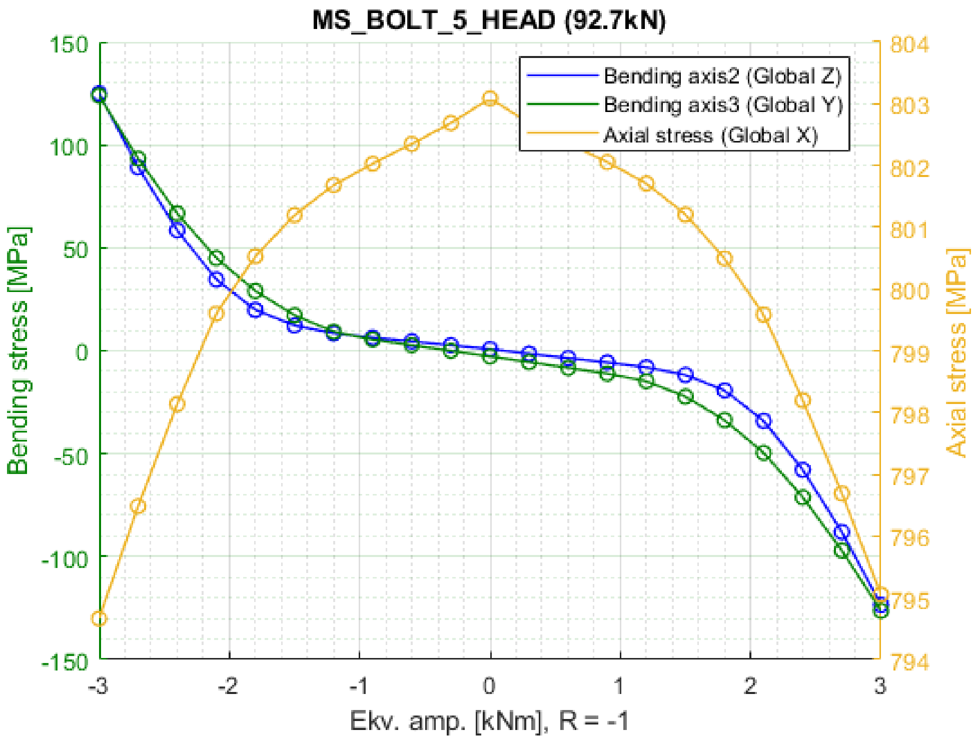

Figure 46: The bending stresses obtained for bolt 5 together with the axial strain for when the friction coefficient is 0.25.

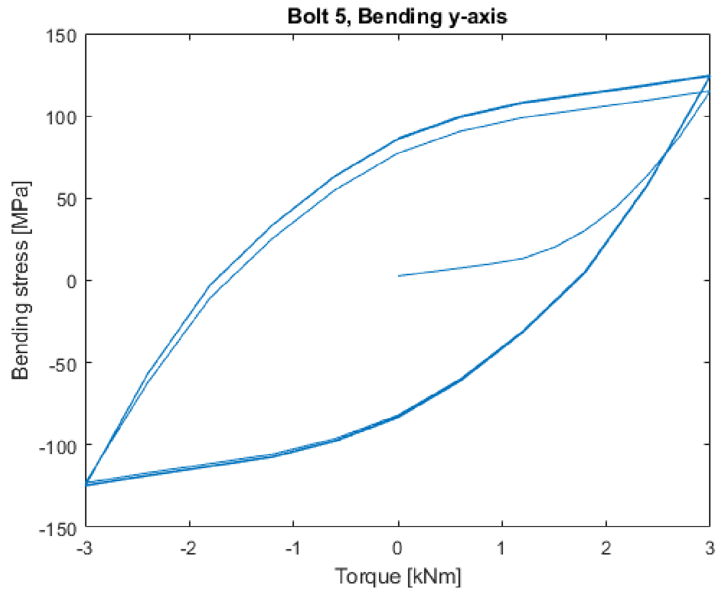

Figure 47: The bending stresses around the y-axis, obtained by the modeled strain gauges for bolt 5 with a friction coefficient of 0.25.

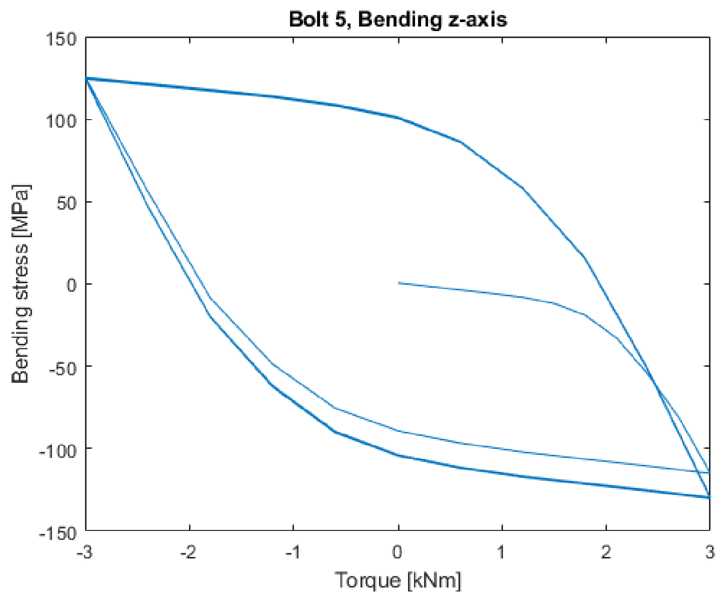

Figure 48: The bending stresses around the z-axis, obtained by the modeled strain gauges for bolt 5 with a friction coefficient of 0.25.

4.2.6 Friction and clamping force

The different combinations used for the friction coefficient and the clamping forces in the simulations is presented below.

4.2.6.1 Friction coefficient: 0.2, pretension force frame bolts: 22.3 kN, pretension force beam bolts: 72.7 kN

The results showing the effects of a reduced clamping force for all of the bolts together with an increased friction coefficient of 0.2 can be seen in Figure 49. The prediction from the simulation is more reasonable when compared to the physical tests for bolt 4. The 100 000-cycle load for bolt 4 is now at 1.88 kNm which is a reduction of 21 %. The load at the acceptance criteria for bolt 5 is however at 2.12 kNm, which is a decrease of 2.7 %.

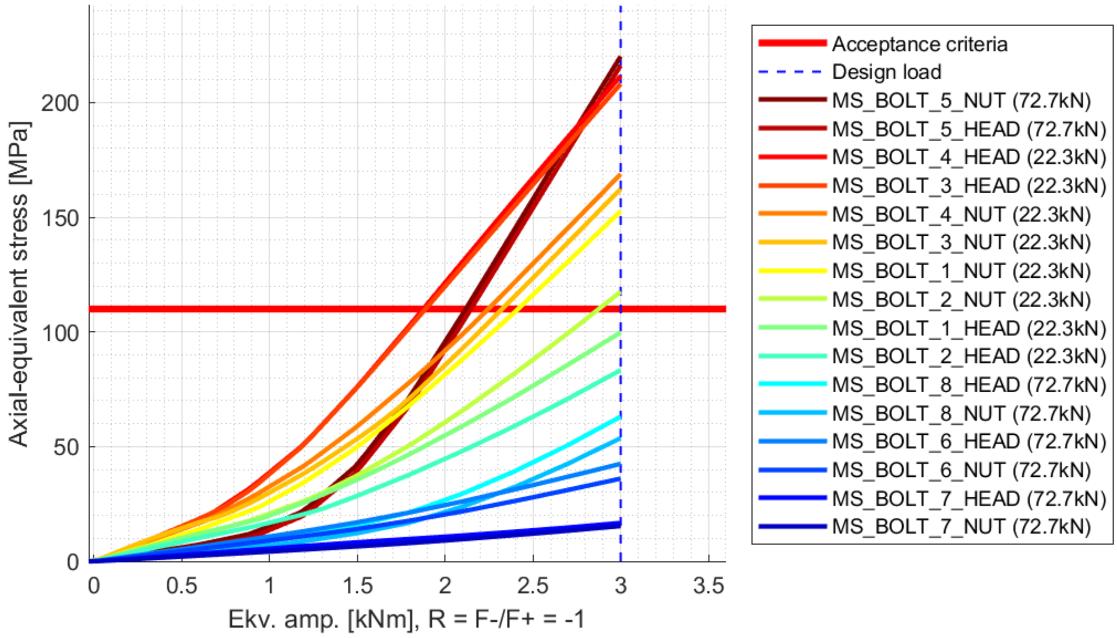

Figure 49: Simulation predictions when the clamping force is reduced according to test results together with an increased friction coefficient of 0.2.

4.2.6.2 Friction coefficient: 0.3, pretension force frame bolts: 22.3 kN, pretension force beam bolts: 72.7 kN

The result obtained by the bolt evaluation script with lower pretension force together with a friction coefficient of 0.3 is presented in Figure 50. The 100 000-cycle load for bolt 4 is at 1.94 kNm, which compared to the standard analysis is a reduction of 19 %. The new load for bolt 5 is at 2.73 kNm which is an increase for the 100 000-cycle load of 25 %.

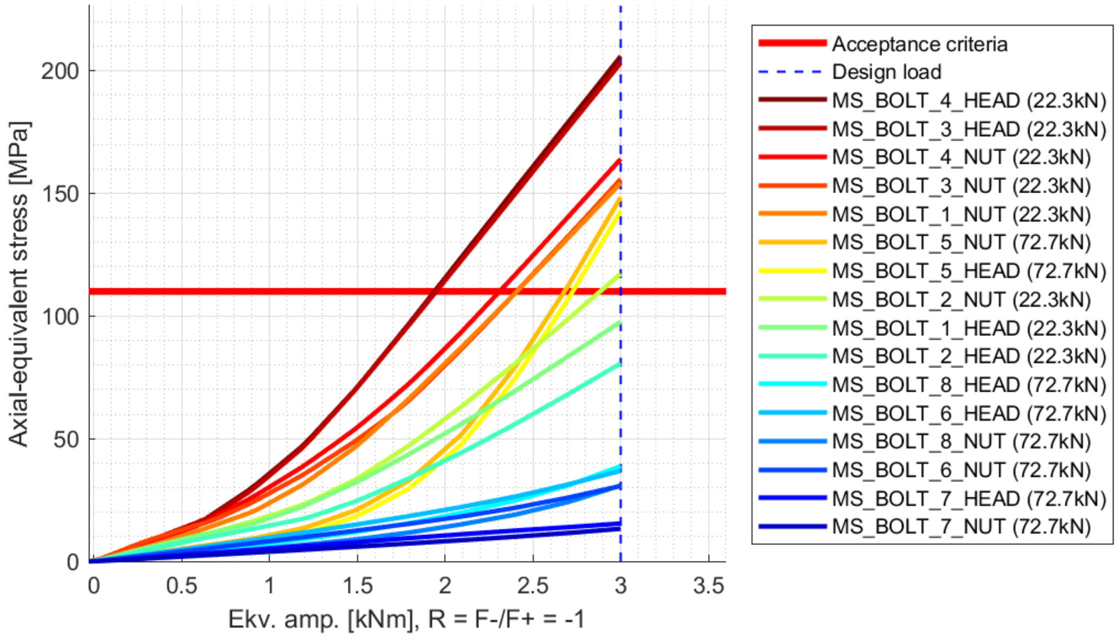

Figure 50: Simulation results for the pretension forces measured after the load series together with a friction coefficient of 0.3.

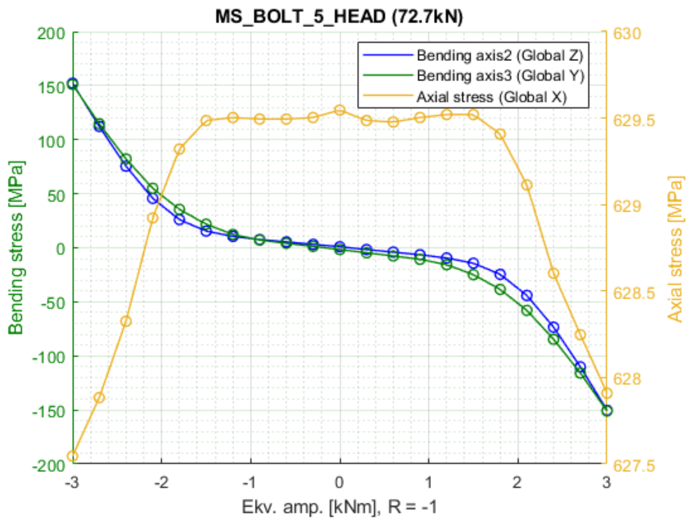

Figure 51: Bending stresses obtained by the bolt script for bolt 5 with a friction coefficient of 0.3.

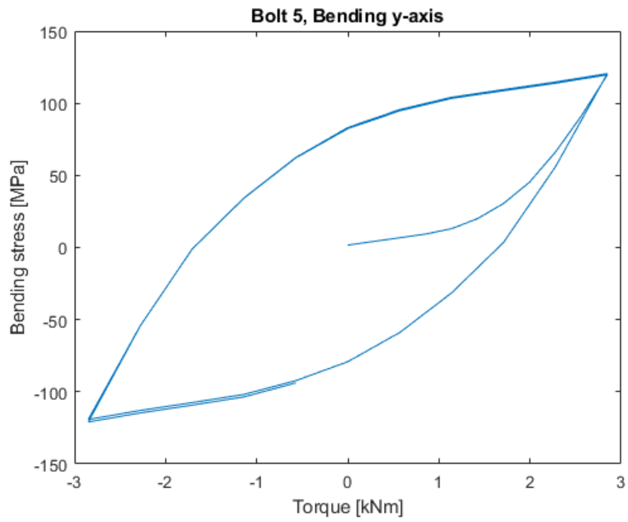

Figure 52: Bending stress around the y-axis for the cyclic simulation with pretension force of 72.7 kN and a friction coefficient of 0.3

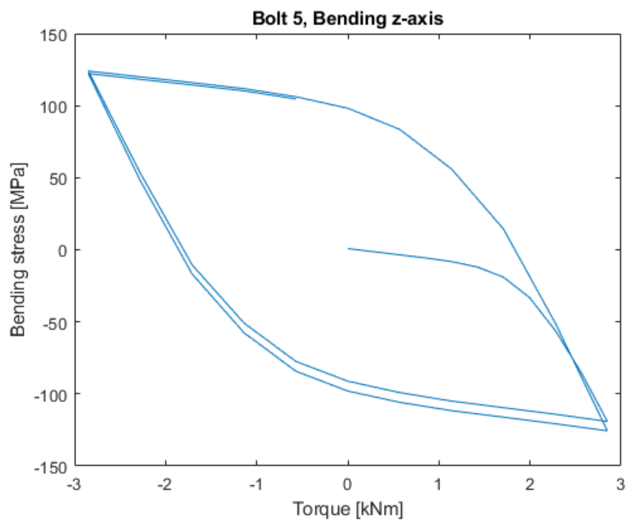

Figure 53: Bending stress around the z-axis for the cyclic simulation with pretension force of 72.7 kN and a friction coefficient of 0.3

In Figure 54 and Figure 55 plots for comparison of the results obtained from the measurements together with the result obtained from simulations is presented. The pretension force used in the simulations is at 72.7 kN. The friction coefficient used in the simulations is 0.15 and 0.3. As can be seen is the correlation improved significantly once the friction coefficient is set to 0.3.

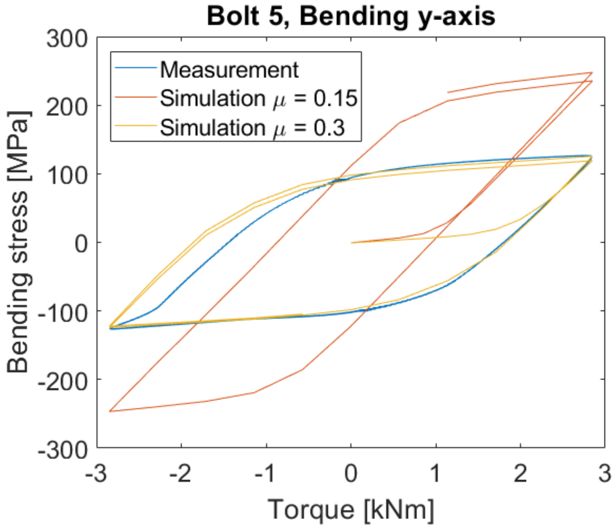

Figure 54: Comparison of the results for bolt 5 obtained from measurement together with the simulation results with a friction coefficient of 0.15 and 0.3 for bending around the y-axis.

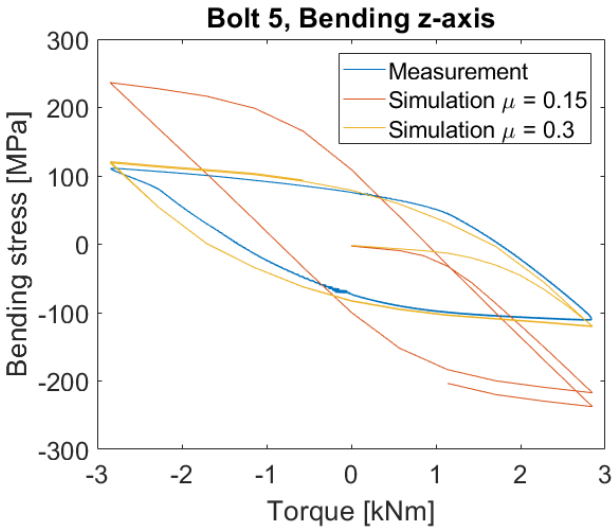

Figure 55: Comparison of the results for bolt 5 obtained from measurement together with the simulation results with a friction coefficient of 0.15 and 0.3 for bending around the z-axis.

4.2.6.3 Friction coefficient: 0.3, pretension force frame bolts: 22.3 kN, pretension force beam bolts: 82.7 kN

The results obtained by the bolt evaluation script for when the pretension forces of the beam bolts are assigned according to the initial measured pretension forces are seen in Figure 56. The prediction for bolt 4 is unchanged while the 100 000 cycle load is calculated to 2.94 kNm for bolt 5.

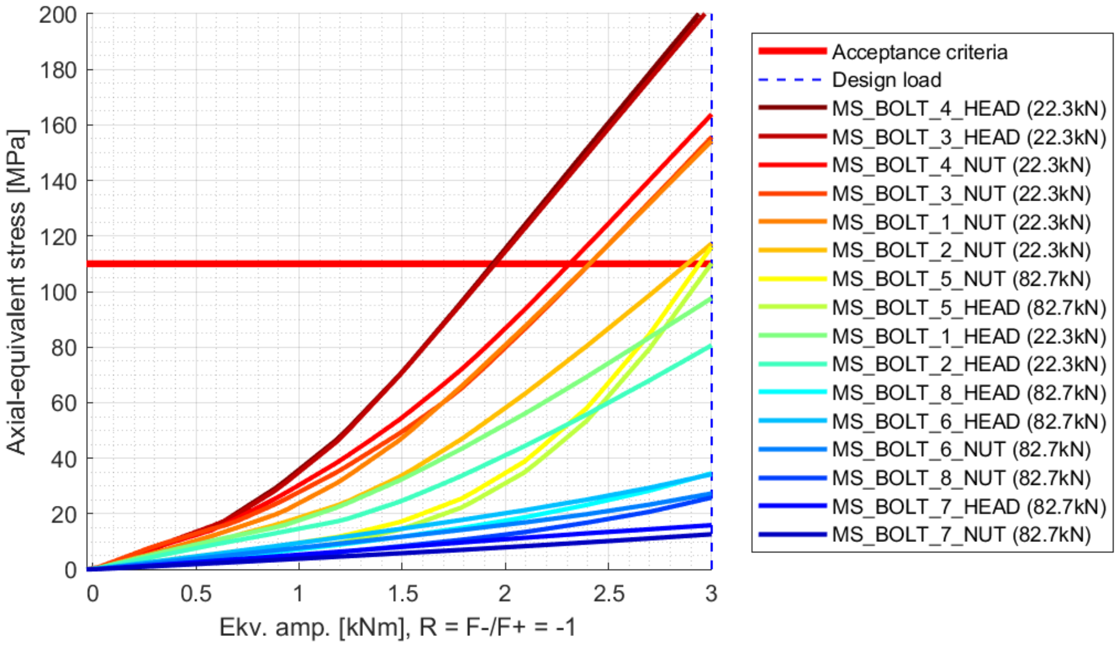

Figure 56: Simulation results for the initial measured pretension forces together with a friction coefficient of 0.3.

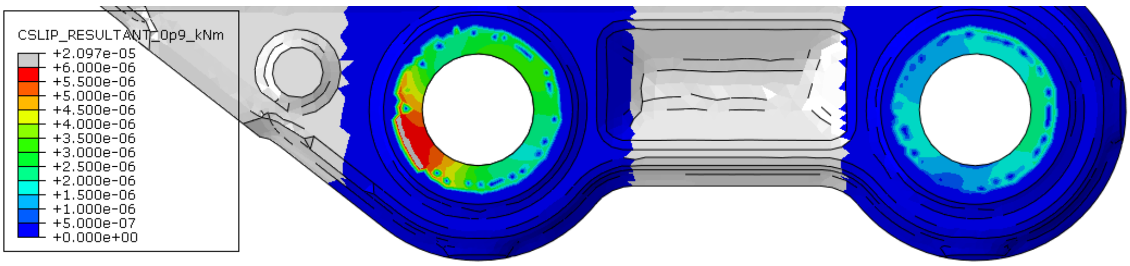

Figure 57: Cslip resultant on the beam bracket for bolt 5 to the left and bolt 6 to the right when the applied torque is 0.9 kNm. NB: The scale is from 0 to $6.0 \cdot 10^{-6}$m

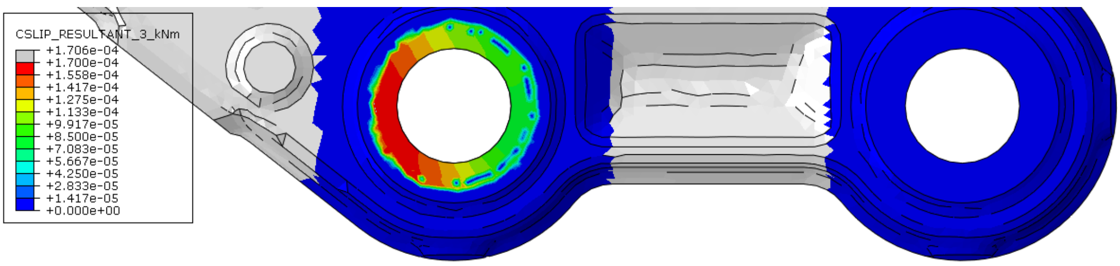

Figure 58: Cslip resultant on the beam bracket for bolt 5 to the left and bolt 6 to the right when the applied torque is 3 kNm. NB: The scale is from 0 to $1.7 \cdot 10^{-4}$m

The prediction for the bolts with an applied pretension force of 22.3 kN for the frame bolts and 82.7 kN for the beam bolts and while the friction coefficient is increased to 0.3, is presented in Figure 59. The model presented in the background is used for this simulation and the clamping lengths of the bolts are according to drawings with a threaded beam bracket. The new 100 000-cycle load for bolt 4 is now predicted to 1.96 kNm while the load for bolt 5 is predicted to 2.81 kNm.

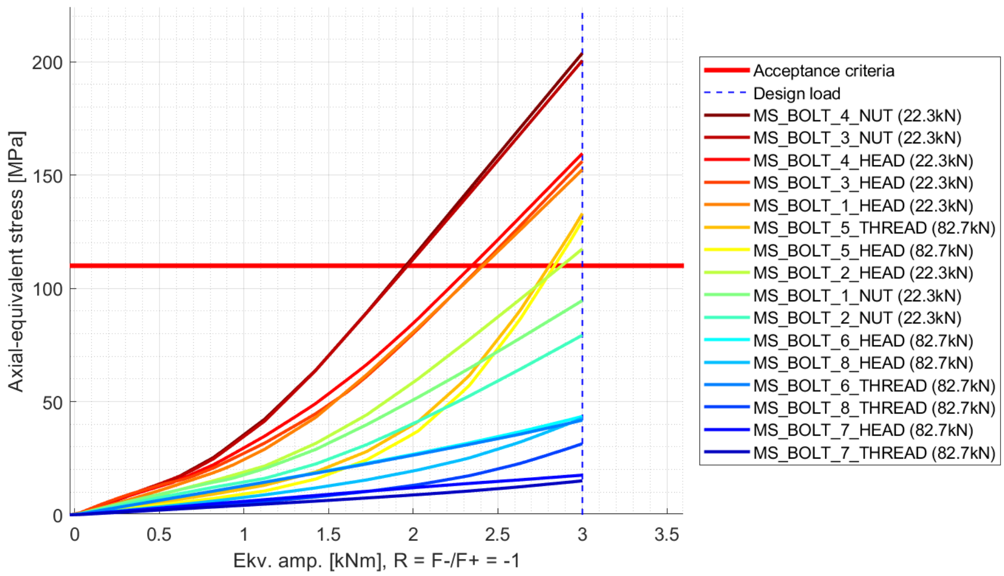

Figure 59: Results obtained by the bolt evaluation script for the simulation model used in the background. Pretension for the beam bolts is assigned according to measurements before testing, pretension for the frame bolts was assigned according to measurements after the load series, and the friction coefficient was set to 0.3.

5 Discussion

5.1 Clamping forces

The pretension forces measured before all tests are at expected magnitudes if the tool and friction variance is taken into account.

The values are extracted for when the torque is zero. If a hysteresis is present for the bolts axial force, the clamping forces will differ depending on which direction the torque is applied. A mean value of these clamping forces are in that case calculated and used as an approximation for the real clamping forces. The data presented for some of the clamping forces from the rig tests should be considered as an estimation of the actual clamping forces present before the tests are initiated.

5.1.1 Frame bolts

The measurements of the clamping forces during the 100 000 cycle test shows that the frame bolts lose much of their clamping force after only 10 000 cycles and the loss continues as the test proceeds. It could also be seen that the frame bolts lose a significant amount of clamping forces during the load series. This loss is probably dependent on the fact that micro slip is present for the frame bolts which leads to wear of the clamped components, which could be seen for the frame in Figure 18. The wear in the frame is clearly viewed and high losses of clamping forces could be present due to this, especially since the clamping length of the frame bolts are only about three times the diameter. According to recommendations from Scania should the length of a bolt be a minimum of two times the diameter of the bolt in order to prevent significant clamping force loss. The wear in the frame bracket is not as significant as for the frame since the paint layer is not as thick on the frame bracket. In the existing method of evaluating bolted joints, the loss of pretension force due to embedment and wear is accounted for by a 10% reduction of the pretension force. Furthermore, there is significant slip present at the head and nut of the frame bolts. The relative movement at the bolts could lead to self-loosening which will reduce the clamping force further.

When clamping forces that better represent the actual clamping forces that are present during the physical tests are used for the frame bolts in the simulations, the 100 000 cycle load is decreased below the calculated value presented in the background as expected. Since the 100 000 cycle load were overestimated in the background for the frame bolts, this means that the correlation is improved.

After the frame bolts have been retightened a couple of times, the pretension forces of bolts 3 and 4 are consistently below the clamping force of bolts 1 and 2. The reason for this is not certain. It could be because of the wear, and the fact that coating might get stuck in the threads of the bolts once they have been retightened a couple of times. Another reason can be that the threads has been deformed.

5.1.2 Beam bolts

The test results show that the beam bolts do not lose significant clamping force during the testing for a torque amplitude between 0.35-2.8 kNm, neither for the load series or during the 100 000 cycle test. Unlike the frame bolts, most of the slip occurring is between the beam brackets and the frame bracket. This means that only a small amount of the relative movement is present at the bolt head and/or nut, which results in self-loosening of the bolts being less likely to occur. Furthermore, the coating of the clamped parts for the beam bolts is not as thick as for the frame. There has, however, been loss of clamping forces in the beam bolts during the tests. This is seen when comparing the clamping force in Table 9 and Table 11. The tests during which losses in clamping forces for the beam bolts were detected, however, were when the frame was not fully fixed to the rig. The mudguard bracket did because of this jump at higher torque amplitudes which could be the reason for the high losses of clamping force. In retrospect, the beam bolts should have been retightened after this was detected.

The measured clamping force for bolt 5 when the data was valid had however decreased to approximately 73 kN. When simulations were performed with a pretension force of 72.7 kN, the correlation to the measured bending stresses becomes worse.

The use of nuts instead of a threaded beam bracket leads to a longer clamping length. The clamping length of bolts 3 and 4 is also increased for the measurements which decreased the negative effects of embedment and wear on the clamping force.

When comparing the bending stresses obtained from the testing to the bending stresses extracted from the bolt evaluation script for bolt 5 further, there are big differences in the stress amplitudes. It can be seen that the amplitude of the bending stress for bolt 5 in the simulations when the standard method was used and with an applied torque of 3 kNm, is approximately 200 MPa in both y- and z-direction, compared to 124 MPa around the y-axis and 109 MPa around the z-axis for the physical test results. Since the simulation method used with the bolt script does not account for the stresses when the torque is relieved as in the testing, there could appear some discrepancy once large slipping is involved.

Running simulations with consecutive load steps did not lead to the stress amplitudes being reduced as expected. The behavior of the bolts is captured in a good sense and the hysteresis is present in a similar manner as for the test results. If comparing the results in Figure 20 and Figure 33 it is seen that once the applied torque is relived from its maximum amplitude, slip is initiated first when the torque changes direction for the physical test results, i.e. when the torque has been relieved by 3 kNm. In the simulation results however, slip is initiated when the torque and has been relieved by 1.9 kNm, this implies that the friction coefficient used between the brackets at bolt 5 in the simulation model and the physical brackets differs, since the pretension forces used are the same.

When the applied pretension force in the simulation is 72.7 kN it can be seen that the 100 000-cycle torque for bolt 5 is reduced. This pretension force could however be unfair to compare against the Wöhler test from the background study due to the following. The beam bolts lose most of their clamping forces during the tests while the rig was loose. However, during the Wöhler tests the beam bolts do not lose any clamping force, as seen in Table 9, the initial pretension forces from the measurements for the beam bolts are at a minimum 82 kN. The 100 000-cycle load is therefore evaluated with a pretension force of 82.7 kN in the simulations to reflect the reality. As such, the loads at the acceptance criteria are increased for the beam bolts seen in Figure 39.

5.2 Friction

When the friction coefficient is increased in the simulations, the bending stresses for bolt 5 are reduced as expected. This depends primarily on the torque can be relieved for a longer time from a maximum and minimum magnitude before slip is initiated as seen for the cyclic simulations. The slope of the curve once slip is fully initiated becomes more aggressive as the friction coefficient is increased and the correlation to the measured bending stresses is improved. The slope of the bending stress for the simulation with a pretension force according to standards and with a friction coefficient of 0.2 is more similar to the bending stresses of the physical test results. Once the pretension forces are reduced to a magnitude that represent the values measured in testing, the friction coefficient has to be set to 0.3 in order for the bending stress of bolt 5 to correlate. The correlation is however improved significantly with this friction coefficient.

The new 100 000 cycle load for bolt 5, when the pretension forces are according to the measured forces before tests are initiated at 82.7 kN and with a friction coefficient of 0.3, is predicted to 2.94 kNm as seen in Figure 56. The prediction for bolt 4 is unchanged with a load of 1.94 kNm at the acceptance criteria.

Finally, a simulation was performed for the original design used in the Wöhler test in the previous study with a pretension force of 22.3 kN for the frame bolts and 82.7 kN for the beam bolts and a friction coefficient of 0.3. The correlation is improved for bolt 4 with a discrepancy of 2 % between the 100 000-cycle load determined from simulation and testing. Bolt 5 is predicted to withstand a load 85 % higher compared to the simulated value from previous calculations in the background. Since bolt 5 did not ever break during the Wöhler test, this is a reasonable change.

5.3 Uncertainties

The bending stresses from the physical tests are calculated from the strain gauges equipped at the circumference of the bolts, which are not exactly aligned with the global coordinates. Since the bolt evaluation script always uses points on the circumference that are exposed to the highest stresses, the comparison could be misleading in the sense that depending on the placement of the strain gauges in the tests so are different stresses obtained. The bending stress amplitudes obtained by the modelled strain gauges do not differ significantly from the stress amplitudes obtained by the bolt evaluation script.

It took several load cycles during the load series to reach the suitable load magnitudes. This could have affected the results in that a lot of embedment, for example, may already have occurred before measurements were collected. In order to better capture this, a cylinder that faster reaches the wanted load amplitude is desirable. Alternatively, data should be collected during the whole process to capture all the changes in the bolts behavior.

Depending on the tolerance of the beam and the beam brackets, two different cases for how the beam brackets encloses the beam could occur. The first case occurs when the beam brackets overclose the beam and the contact is at the center. For the second case, the beams radius is bigger compared to the brackets. This results in contact at the top and bottom of the beam brackets. This could result in different initial bending stresses for the beam bolts and also affect the pretension force depending on which case is used.

6 Conclusion

- The simulation method captures the behavior of the bolts in a good way once input values such as friction coefficients and pretension forces are adjusted.
- Once parameters are used that represent the measurements regarding the pretension forces and friction coefficient, the correlation is improved significantly.
- The tests implies that significant loss of clamping force is found due to wear and self-loosening of the frame bolts after only a few cycles.
- Bolt 5 was exposed to bending stresses mainly due to slip between the clamped components. This lead bolt 5 to be very sensitive to friction coefficient adjustment.
- The method do captures changes in parameters well and according to expectations.
- A generalized suggestion on how to improve the method is difficult to give since the findings of the parameters are mainly relevant for this specific construction.
- Evaluate the pretension force reduction of 10 % used in the existing method.
- Further investigations should be done to get an understanding of how to better predict the loss of pretension forces of the bolts.
- Evaluate friction coefficient used for the existing method. More investigations on which friction coefficients that should be used for different types of materials and coatings could be advised.

7 References

[1] Henningsen, D. (2018). *Wöhler test Mudguard Bracket.* Södertälje: Scania. 7049991.

[2] Heed Elvegård, E. (2018). *Evaluation of bolt analysis script with FEM. Example, Mudguard Bracket.* Södertälje: Scania. 7054348.

[3] Österlöf, R. (2017). *Best practice for bolt analysis with the finite element method.* Södertälje: Scania. 7028696

[4] Huang, A. (2014). *Böjutmattning av Skruv,* KTH. Hållfasthetslära.

[5] Skogsmo, J. (2014). *Swedish Fasteners Network*. [Online]. Available: http://extra.ivf.se/sfn_handbok/template.asp?lank=160. [Accessed May 27, 2019].

[6] Dassault Systemes. (2016). *Abaqus 6.13 Documentation.* [Online]. Available: http://dsk.ippt.pan.pl/docs/abaqus/v6.13/index.html. [Accessed June 4, 2019].

8 Appendix

Table 12: Summary of the simulation results for bolt 4 .

Bolt 4	Standard method	Lower pretension force	$\mu = 0.2$	$\mu = 0.25$	Lower pretension, $\mu = 0.2$	Lower pretension, $\mu = 0.3$
Axial stress amplitude [MPa]	37	78	35	34	78	76
Bending stress amplitude around x-axis [MPa]	182	211	170	161	200	189
Bending stress amplitude around z-axis [MPa]	55	65	61	64	76	83
100 000 cycle load for axial equivalent stress [kNm]	2.39	1.83	2.47	2.54	1.88	1.94

Table 13: Summary of the simulation results for bolt 5.

Bolt 5	Standard method	Pre-force = 72.7 kN	Pre-force =82.7 kN	$\mu = 0.2$	$\mu = 0.25$	Pre-force = 72.7 kN $\mu = 0.2$	Pre-force = 72.7 kN $\mu = 0.3$	Pre-force = 82.7 kN $\mu = 0.3$
Axial stress amplitude [MPa]	10	4	6	5	4	4	1	2
Bending stress amplitude around y-axis [MPa]	207	253	226	158	125	223	150	120
Bending stress amplitude around z-axis [MPa]	207	284	254	158	125	235	150	126
100 000 cycle load for axial equivalent stress [kNm]	2.18	1.83	1.98	2.57	2.88	2.12	2.73	2.94

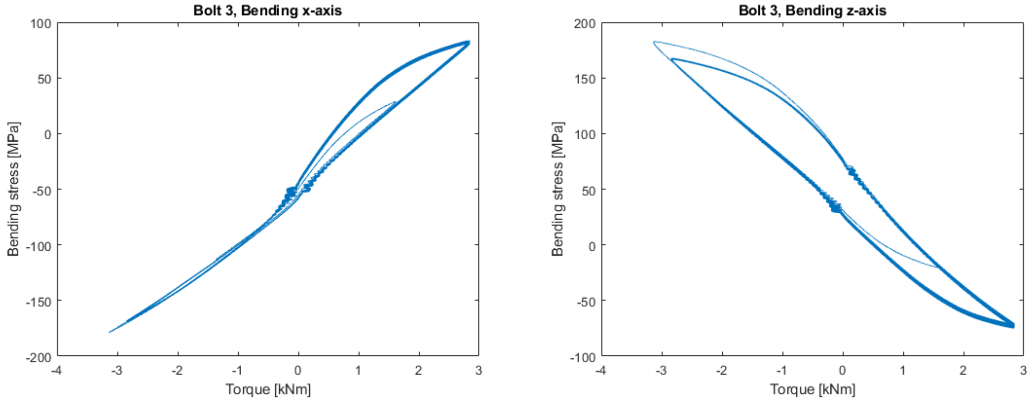

Figure 60: Bending stresses for bolt 3 from the physical test with an applied torque of 2.8 kNm.

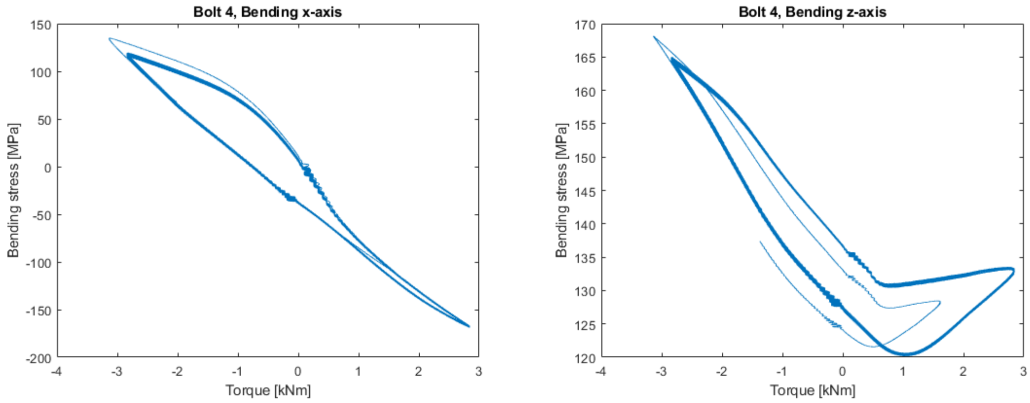

Figure 61: Bending stresses for bolt 4 from the physical test with an applied torque of 2.8 kNm.

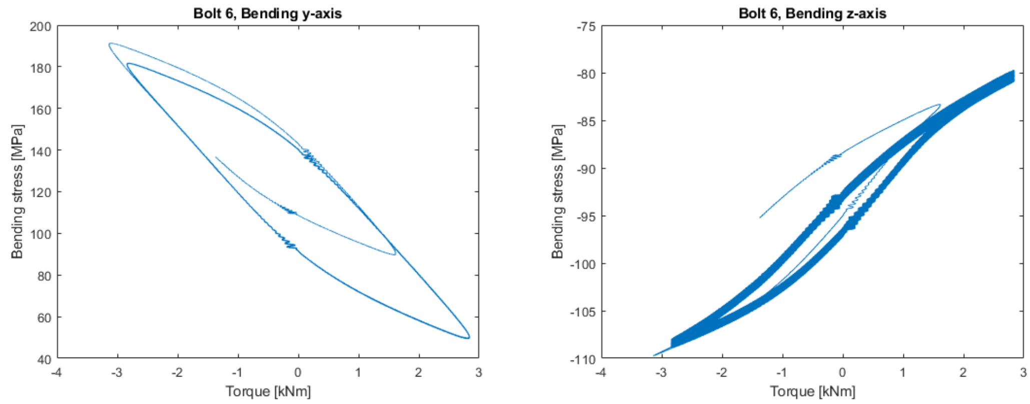

Figure 62: Bending stresses for bolt 6 from the physical test with an applied torque of 2.8 kNm.

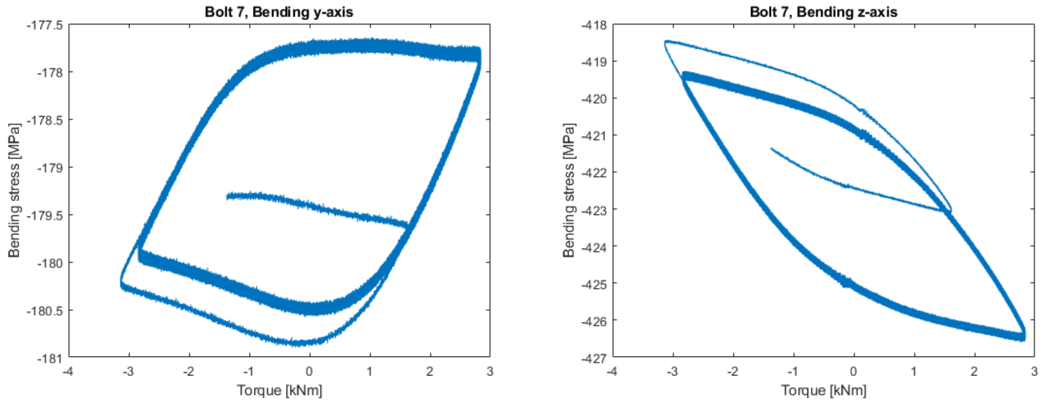

Figure 63: Bending stresses for bolt 7 from the physical test with an applied torque of 2.8 kNm.

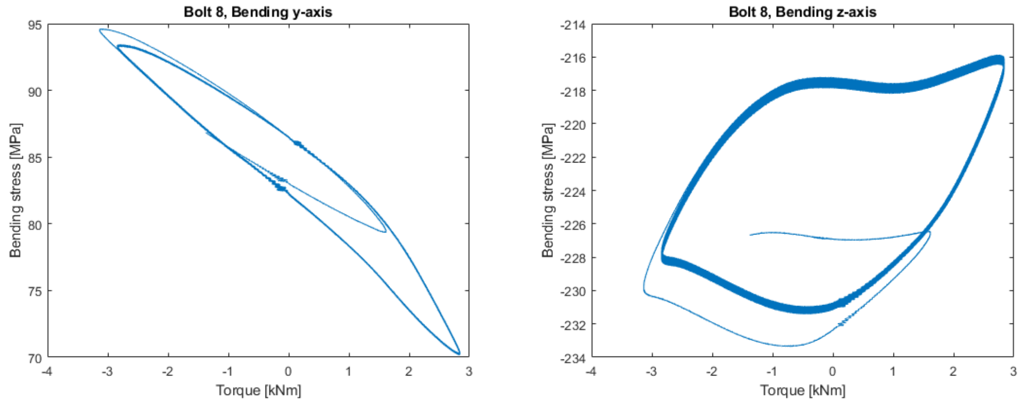

Figure 64: Bending stresses for bolt 3 from the physical test with an applied torque of 2.8 kNm.

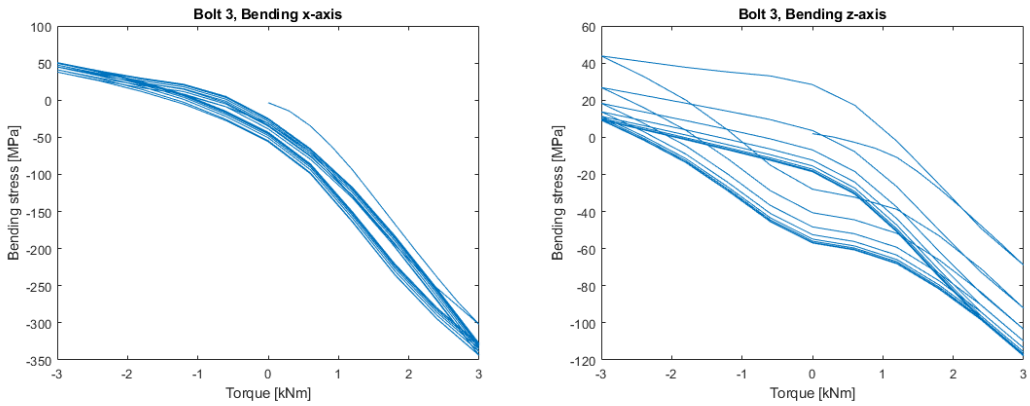

Figure 65: Bending stresses for bolt 3 from the simulation for a torque of 3 kNm, 42.3 kN in pretension force and $\mu = 0.15$.

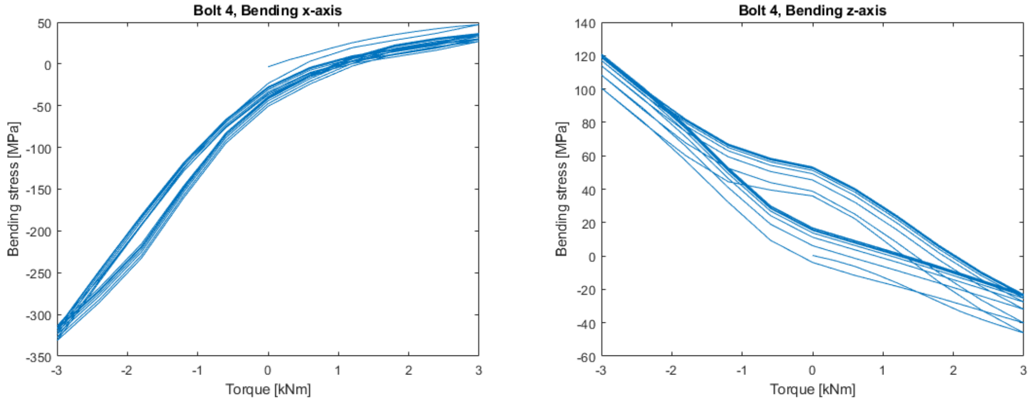

Figure 66: Bending stresses for bolt 4 from the simulation for a torque of 3 kNm, 42.3 kN in pretension force and $\mu = 0.15$.

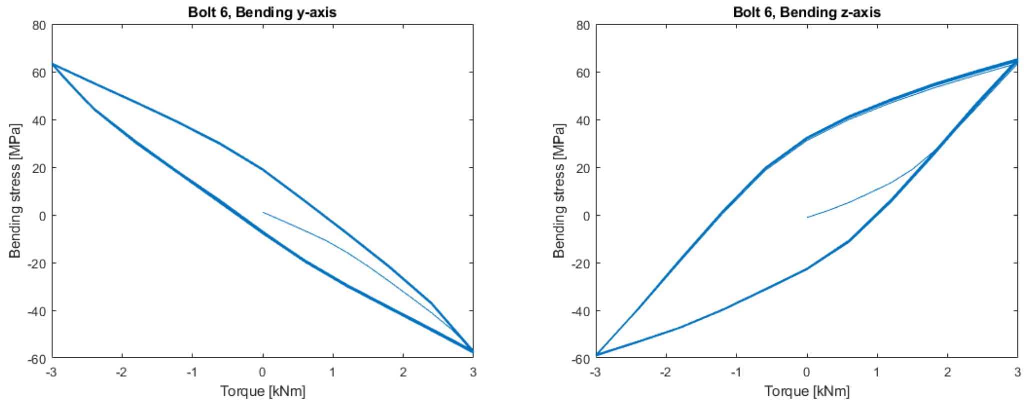

Figure 67: Bending stresses for bolt 6 from the simulation for a torque of 3 kNm, 92.7 kN in pretension force and $\mu = 0.15$.

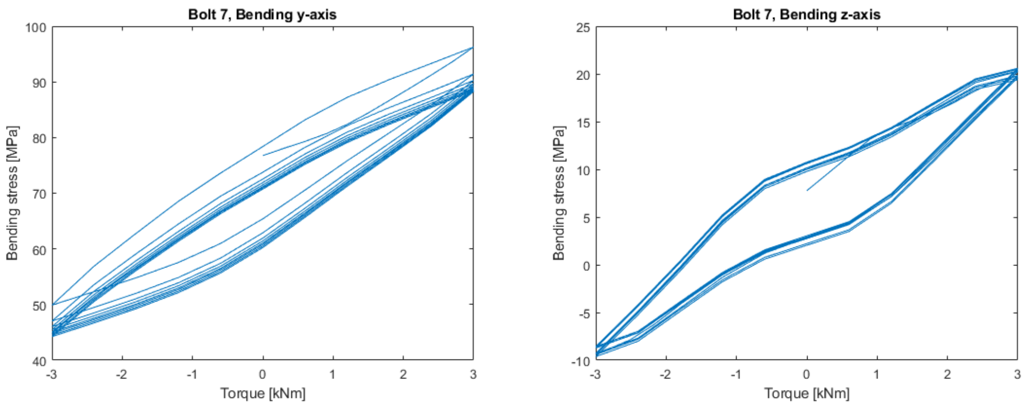

Figure 68: Bending stresses for bolt 7 from the simulation for a torque of 3 kNm, 92.7 kN in pretension force and $\mu = 0.15$.

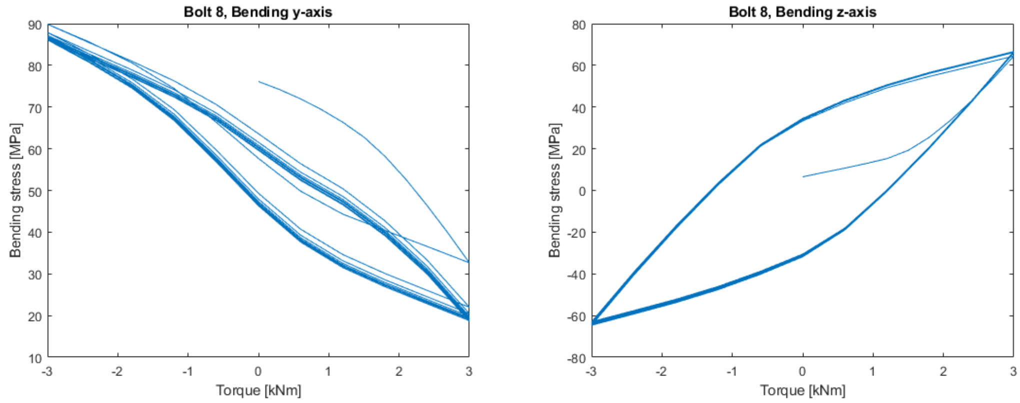

Figure 69: Bending stresses for bolt 8 from the simulation for a torque of 3 kNm, 92.7 kN in pretension force and $\mu = 0.15$.

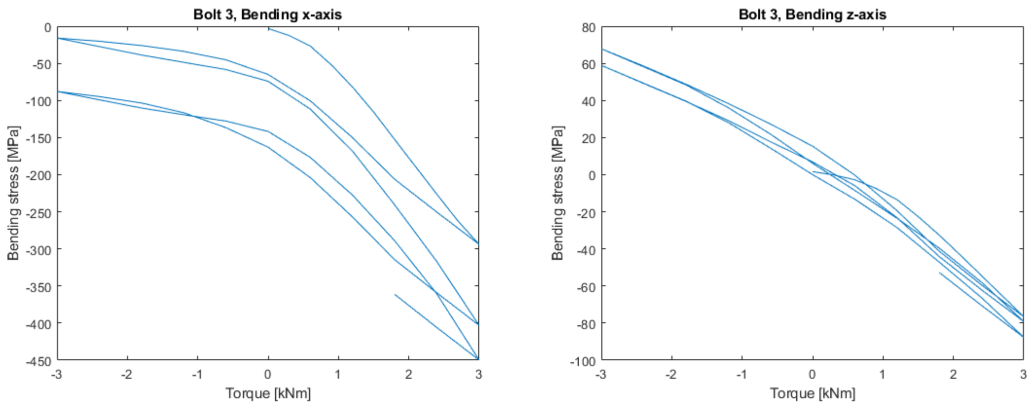

Figure 70: Bending stresses for bolt 3 from the simulation for a torque of 3 kNm, 22.3 kN in pretension force and $\mu = 0.3$.

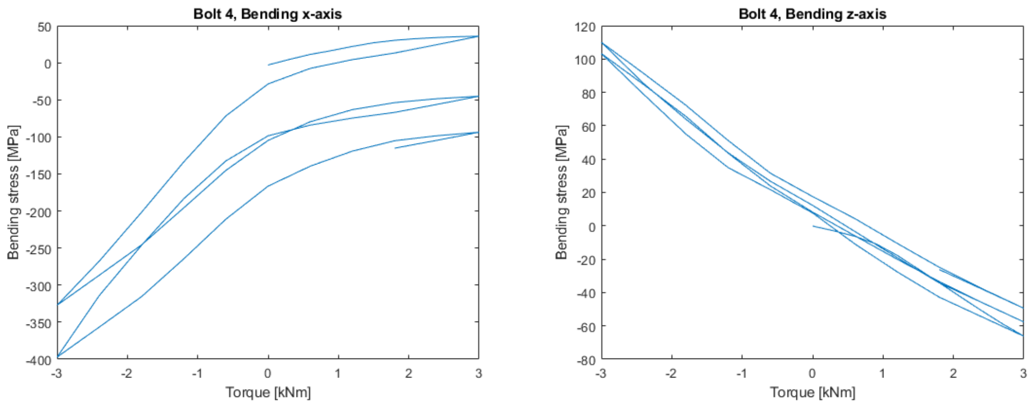

Figure 71: Bending stresses for bolt 4 from the simulation for a torque of 3 kNm, 22.3 kN in pretension force and μ=0.3.

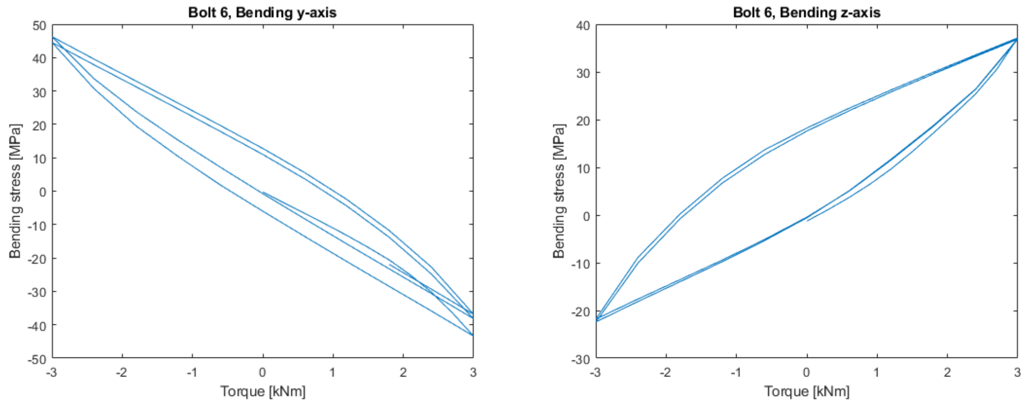

Figure 72: Bending stresses for bolt 6 from the simulation for a torque of 3 kNm, 72.7 kN in pretension force and μ=0.3.

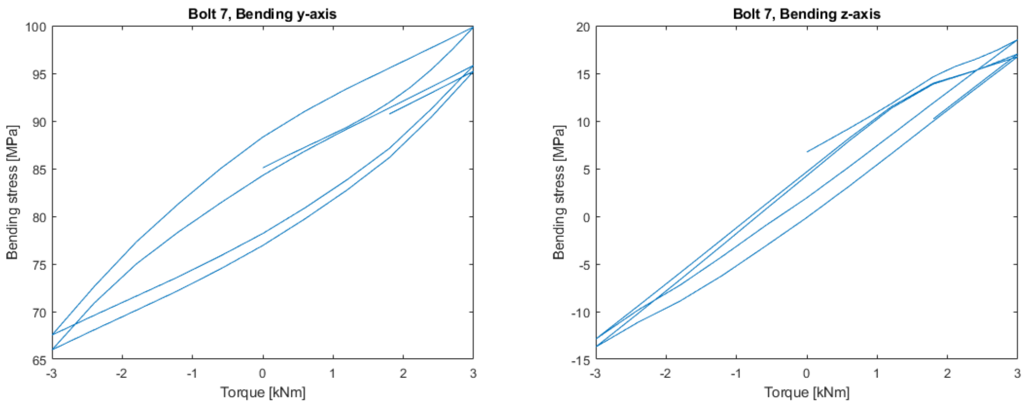

Figure 73: Bending stresses for bolt 7 from the simulation for a torque of 3 kNm, 72.7 kN in pretension force and μ=0.3.

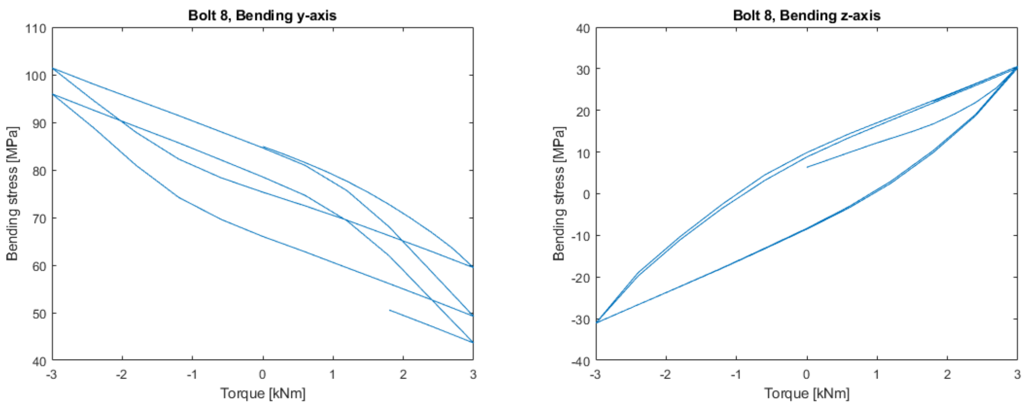

Figure 74: Bending stresses for bolt 8 from the simulation for a torque of 3 kNm, 72.7 kN in pretension force and μ=0.3.